ARR No. L5H23

NATIONAL ADVISORY COMMITTEE FOR AERONAUTICS

WARTIME REPORT

ORIGINALLY ISSUED

December 1945 as
Advance Restricted Report L5H23

THE EFFECT OF CONCENTRATED LOADS ON FLEXIBLE RINGS IN CIRCULAR SHELLS

By Paul Kuhn, John E. Duberg, and George E. Griffith

Langley Memorial Aeronautical Laboratory
Langley Field, Va.

NACA

WASHINGTON

NACA ARR No. L5H23

NATIONAL ADVISORY COMMITTEE FOR AERONAUTICS

ADVANCE RESTRICTED REPORT

THE EFFECT OF CONCENTRATED LOADS ON FLEXIBLE RINGS IN CIRCULAR SHELLS

By Paul Kuhn, John E. Duberg, and George E. Griffith

SUMMARY

The standard method of analyzing fuselage rings has been known for some time to be considerably in error when the rings are flexible, as is usually true of secondary rings in large fuselages. In order to provide a basis for a more accurate analysis, strain measurements were made on a series of circular cylinders with reinforcing rings, subjected to concentrated loads, in which the bending stiffness of the rings was varied systematically over a wide range. The results are presented and compared with the results obtained by theoretical methods. A method proposed by N. J. Hoff for analyzing rings subjected to vertical loads, extended in the present paper to cover all basic cases, was found to give satisfactory agreement with the test results. A method proposed by Wignot, Combs, and Ensrud was found to be considerably in error when used in the originally published form. A modification of this method was developed with the relative stiffness parameter redefined, and the accuracy of the method was thereby improved appreciably. This modified method, although less accurate than the method of Hoff, retains the advantage offered in the original method of Wignot, Combs, and Ensrud of greatly reducing the time of analysis through the use of graphs.

INTRODUCTION

The so-called secondary rings in fuselage shells are usually analyzed on the basis of the assumption that the shear stresses in the skin which balance the load applied to the ring are distributed in accordance with the

standard engineering theory of bending. For a radial load applied to a ring in a shell of circular cross section, for instance, this theory gives a shear stress that is zero at the load and increases to a maximum at the neutral axis 90° from the load. It has been recognized for some time, however, that this basic assumption may not agree very well with the facts. The secondary rings are relatively flexible, and intuition alone is sufficient to indicate that a concentrated load applied to a flexible ring will cause local concentrations of stress near the load. Some designers consequently assume a triangular distribution of the skin shears; others, a uniform distribution, which is between the triangular distribution and that given by the standard theory. This uncertainty about the distribution of the shear stresses causes a corresponding uncertainty in the calculation of the maximum shear stresses in the skin. In addition, it causes an even greater uncertainty in the calculation of the bending moments in the rings. Strain measurements on the rings of actual large fuselages have shown ring bending stresses that were only a small fraction (less than one-fifth) of the values calculated by the standard method.

The investigation reported herein was undertaken in order to provide a more secure basis for the analysis of rings. Systematic strain measurements were made on a number of cylinders having rings with widely differing flexibilities and were compared with the analytical results obtained from two theories. The theories were extended to increase their usefulness or modified to increase their accuracy.

SYMBOLS

A, B	coefficients defined in table 4
C, D	Fourier coefficients for distributed load
E	Young's modulus, psi
G	shear modulus, psi
H	axial force in ring, pounds
I	moment of inertia of cross section, inches^4
K	shear-stiffness constant used in reference 3

L	spacing of rings, inches (note that in equations (3), (4), and (5), the symbols L and L_o have special meanings and definitions discussed in connection with these equations)
M	bending moment in ring, inch-pounds
P	radial load, pounds
Q	static moment about neutral axis of cross-sectional area lying between extreme fiber and plane under consideration
R	radius of cylinder
T	tangential force acting on ring, pounds
U	internal work, inch-pounds
V	shear force, pounds
C_M	coefficient of bending moment in ring (M/PR) or (M/TR)
C_q	coefficient of shear flow in skin (qR/P)
a, b	Fourier coefficients for C_M, C_q, and σ
d	relative stiffness parameter used in reference 3; see equations (2), (4), and (4a) for discussion and definition
i	general number of bay or ring
n	general number of Fourier coefficient
q	shear flow (running shear), pounds per inch
t	thickness of skin, inches
t'	thickness of all material carrying bending stresses in cylinder if uniformly distributed around perimeter, inches
x	distance from tip of cylinder, inches
γ	shear strain
σ	longitudinal normal stress in skin, psi

τ shear stress in skin, psi

φ angular distance of given point on ring from point of application of concentrated load

Subscript:

R rigid

TEST SPECIMENS AND PROCEDURES

Test specimens.- The test specimens were four circular cylinders of 24S-T aluminum alloy reinforced by four equally spaced rings. The main dimensions are given in table 1. Cylinders 1, 2, and 3 formed a series in which all dimensions were nominally equal except the moments of inertia of the rings, which were varied approximately as 1:10: 100. Cylinders 1a, 1b, and 1c were modifications of cylinder 1. Cylinder 4 had rings of the same cross section as cylinder 2 but twice the skin thickness. Pertinent details of construction are shown in figures 1 and 2. It will be noted that the cross-sections of the rings were made symmetrical about the skin in order to avoid consideration of the amount of skin working with the rings.

Test procedures.- The main tests consisted in applying a radial load to each ring in turn and measuring the bending stresses in the loaded ring as well as in the two adjacent rings. Shear stresses were measured in the skin adjacent to the tip ring and to the middle ring. In one test, a tangential load was applied to the tip ring of a shortened cylinder. On cylinder 1, the radial load was outward and was produced by dead weights. On all other cylinders, the radial load was inward and was produced by a hydraulic jack used in conjunction with a dynamometer accurate to about 1/2 percent. Careful check tests made on cylinder 1 with both methods of loading showed no measurable difference, as was expected.

The bending stresses in the rings were computed from measurements with Baldwin-Southwark SR-4 electric strain gages, types A-1 and A-5 (gage lengths 13/16 and 1/2 inch, respectively). The shear stresses in the skin were computed from measurements with Baldwin-Southwark SR-4 electric gage rosettes, type AR-1. All gages were used in

pairs back-to-back. For converting strains to stresses, Young's modulus was taken as 10.6×10^3 ksi and the shear modulus as 4.00×10^3 ksi.

From preliminary readings of the gages near the point of load application, an estimate was made of the load necessary to produce a maximum stress of about 20 ksi in the ring. In the actual test, the chosen load was applied in five equal increments. Load-strain plots were made for the gages near the load and for all rosettes. It was found that all points except the one at zero load fell very close to a straight line in each case; the deviation of the zero load point from the straight line was never larger than about 1×10^{-5}. The strain readings are believed to be accurate to better than 2 percent in all cases.

METHODS OF ANALYSIS

Standard method.- The analysis of fuselage rings is usually based on the assumption that the skin shears balancing the applied loads are distributed in accordance with the elementary theories of structures. In the specific case of a radial load, the skin shears are assumed to follow the familiar VQ/I formula, which gives for the circular cylinder

$$\tau t = q = \frac{P}{\pi R} \sin \varphi \qquad (1)$$

When the skin shears have been computed by formula (1), they may be considered as external loads applied to the ring, and the ring can be analyzed by any applicable method of dealing with statically indeterminate structures. For a number of basic cases that are encountered frequently, the results of such analyses have been published in the form of tables or graphs of coefficients; graphs for the circular ring with a radial load have been given, for instance, in reference 1. Tables and graphs of this kind are of very material aid in reducing the labor of analysis.

Hoff's method.- The use of formula (1) for computing the skin shears implies the assumption that the stiffness of the ring is very large compared with the stiffness of the skin. Secondary fuselage rings, however, are often relatively flexible and deform to such an extent that the shear stresses in the supporting skin are altered; the standard method of analysis consequently becomes inaccurate. A more precise method of analysis must take into account the interaction between a flexible ring and the supporting skin. One solution of this problem was given by Hoff in reference 2. Hoff considered the action of a circular cylinder, cantilevered from a rigid base, with two equal vertical forces equidistant from the vertical diameter applied to the tip ring. He assumed that the important stresses are the bending stresses in the ring, the shear stresses in the skin, and the longitudinal stresses in the skin, including stringers if present. All three of these stress systems were expressed by related Fourier series, and the coefficients of the Fourier series were obtained by the principle of Least Work. An extension of Hoff's method to the cases of a radial load, a tangential load, or a moment load applied at any ring is given in the appendix.

Hoff's method gives a fairly complete and entirely rational answer to the problem. The slight lack of completeness resulting from the simplifying assumptions is unlikely to be of practical importance. More serious is the objection that the method requires computations that are very tedious, at least compared with the standard method.

Method of Wignot, Combs, and Ensrud.- The most essential features of the method of Wignot, Combs, and Ensrud (reference 3) may be described briefly as follows. Only the ring directly subjected to an external load was assumed to be affected. The shear stress in the skin adjacent to this ring was assumed to be proportional to the tangential deflection of the ring with respect to a fictitious ring some distance away that does not deform. On the basis of these assumptions, a differential equation for the bending moments in the ring was derived and solved. The final results were presented in the form of graphs as functions of a parameter d that relates the shear stiffness K of the skin to the bending stiffness EI of the ring by means of the expression

$$d = \frac{KR^3}{EI} \qquad (2)$$

The curves of Wise (reference 1) computed by the standard method appear on these graphs as the limiting case of rigid rings or $d = 0$.

The method has the very desirable feature of simplicity of application; the analysis by means of the graphs given is essentially as simple as the analysis by the standard method with the aid of the graphs of reference 1. It has, however, two obvious defects: one is that it gives no stresses in the rings adjacent to the loaded ring, and these stresses may be of appreciable magnitude; the other is that the theory leaves the numerical value of d indeterminate, because it does not contain any method for deriving the value of K which appears in expression (2). It is stated in reference 3

> "The evaluation of d depends upon the accurate determination of K, for which further development, supplemented by tests, is clearly needed."

Pending such development, this reference suggests that

> "K may be approximated as
>
> $$K = \frac{RtG}{L} \tag{3}$$
>
> where L is the distance along the shell to a section which is not distorted from a circle."

With this approximation for K, the expression for d becomes

$$d = \frac{GtR^4}{EIL} \tag{4}$$

This expression, however, still does not constitute the solution of the problem of determining d, because the theory itself gives no clue as to the magnitude of L. In reference 3, this difficulty was overcome by making an assumption as follows:

> "R/L is assumed to be never less than unity . . . This approximation for K seems justified for any large fuselage comparable with that of the Lockheed Constellation or Boeing Model XB-29 since it gives good test agreement for those airplanes."

Strictly speaking, of course, the inequality $\frac{R}{L} \geq 1$ does not define L. The next expression given in reference 3 indicates, however, that R/L was actually assumed to be equal to unity and with this assumption

expression (4) defines the relative stiffness parameter d as

$$d = \frac{GtR^3}{EI} \qquad (4a)$$

A detailed comparison of the ring theory as developed in reference 3 reveals that it is the limiting case of the theory of reference 2, in which only one ring is considered and the stringers reinforcing the shell are assumed to be infinitely stiff. The assumption of rigid stringers makes it possible to express the shear stresses as proportional to the tangential deflections of the ring. In cylinders of practical proportions, however, the deformations of the stringers have a large influence in defining the shear stresses in the skin and in general tend to decrease them. The smaller shear stresses result in larger maximum bending moments in the ring.

Modified method of reference 3.- The speed with which an analysis can be made by means of the graphs in reference 3 makes this method highly desirable in practical applications. The objection that the method gives no stresses in the rings adjacent to the loaded ring could perhaps be overcome sufficiently to satisfy the demands of practical stress analysis by some empirical or semiempirical method. A preliminary comparison of the test results obtained in the present investigation with the results obtained by use of reference 3 showed, however, a lack of agreement that supported the objections to the assumptions of this theory mentioned in the last paragraph of the preceding section. The statement in reference 3 that there was good test agreement for two large airplanes could not be checked because the test evidence was not presented. The good test agreement might have been achieved in spite of the defects of the theory by use of an incorrect amount of skin working with the ring. Very little is known at present about the amount of skin working with an actual fuselage ring and consideration of this factor might have an appreciable effect on the calculation of the stresses. In the present investigation, this difficulty was not encountered because the rings were symmetrical about the skin.

Further study of the test results presented herein and of the graphs of reference 3 showed that it was generally possible to match any experimental curve with a curve from the proper graph. This observation led to

the thought that closer correlation between test and calculation might be achieved if the method of determining d were modified. Such a modification would be in line with the remark in reference 3 quoted previously that "further development, supplemented by tests, is clearly needed." On the basis of general physical considerations, it was decided to retain expression (4) for determining d but, instead of assuming L to be equal to R, to use a value of L defined by

$$L = L_o\left(1 + \frac{GtL_o^2}{Et'R^2}\right) \qquad (5)$$

In this expression, L_o is the distance from the loaded ring to the actual rigid base, and t' is the thickness of a fictitious "stringer-skin" with a cross-sectional area equal to the sum of the stringer areas and the part of the skin area that is effective in resisting longitudinal stresses.

RESULTS AND DISCUSSION

General remarks.- The results of the investigation are presented in figures 3 through 30 in the form of plots of moment coefficient or skin shear coefficient against developed perimeter of the cylinder. Because of the symmetry of the structure, only one-half of the perimeter needed to be shown. For the moment coefficients, each test point shown represents the average of the two points taken in the left and right side of the cylinder; the two corresponding points always agreed so closely that it was impractical to show them separately. For the shear coefficients individual test points are shown. Computed curves are shown for three of the methods discussed under "Methods of Analysis:" the standard method, Hoff's method (extended where necessary), and the modified method of reference 3. No curves are shown for the unmodified method of reference 3 because the agreement with the experimental data is very poor compared with the results obtained by the modified method or by Hoff's method. On all figures showing data on cylinders 1, 1a, 1b, and 1c, the load is shown acting inward although it was actually acting outward as discussed in the section "Test Procedures." This change was made in order to have all results

similarly presented without being in conflict with the sign conventions given in the appendix. The change should not be objectionable because the check tests showed no difference between an inward-acting and an outward-acting load. (See section on "Test Specimens and Procedures.")

Bending-moment coefficient.- The bending-moment coefficient C_M shown in figures 3 to 21 is defined by the equation

$$M = C_M PR \tag{6}$$

Inspection of the figures shows that the curves computed by Hoff's method with six Fourier coefficients are, on the whole, in very satisfactory agreement with the experimental results if the immediate vicinity of the load is disregarded temporarily. The modified method of reference 3 shows poorer agreement with the test data than Hoff's method in some cases (note, for instance, magnitude and location of the secondary maximum on figures 7, 11, and 15).

Because the curves for the tests with radial load are very steep in the neighborhood of the maximum moment at the load, it is difficult to make comparisons on small-scale figures. A comparison in tabular form is therefore provided in table 2 for these tests. The experimental values of maximum C_M given in this table were obtained from the curves faired through the experimental points and extrapolated to the position of the load. The steepness of the curves combined with the scatter of the test points results in some uncertainty about the maximum values of C_M. Every possible effort was made to reduce this uncertainty by careful choice of scales and accurate plotting, and it is believed that the maximum values of experimental C_M are accurate to within ±5 percent.

If the experimental values of maximum C_M are assumed to be accurate, the errors by Hoff's method range from 20 percent unconservative to 7 percent conservative and the errors by the modified method of reference 3 from 20 percent unconservative to 18 percent conservative. The moment coefficients computed by the standard theory are more than three times as high as the experimental values in the worst case; the coefficients computed by the unmodified method of reference 3 on the other hand, are as low as one-half of the experimental values.

The results of the test made with a tangential load are shown in figure 22. The agreement with Hoff's theory and with the modified theory of reference 3 is again quite satisfactory.

No tests were made with a concentrated moment load. Inspection of the theoretical curves for this loading case shows that the moment decreases very rapidly with increasing distance from the load; and the experimental check is consequently very sensitive to small errors in location of the gage or of the concentrated moment. Furthermore, it is very difficult to introduce a moment in truly concentrated form. Inspection of the moment curves given in reference 3 led to the conclusion that the probable experimental errors would obscure the effect of ring flexibility to such an extent that the test would not be worth while.

The theory indicates that the bending-moment coefficient in an actual structure is always less than that given by the standard elementary theory. In a qualitative way, it may be stated that this coefficient approaches that given by the standard theory as the stiffness of the ring relative to the surrounding part of the shell increases. Experimental results bear out this theoretical conclusion. A comparison of the experimental coefficients in table 2 shows, for instance, that the loaded tip rings (ring 1) of cylinders 1, 2, and 3 have consecutively higher coefficients because the moments of inertia increase in this order. Similarly, the coefficient for the tip ring of cylinder 4 is less than that for the rip ring of cylinder 2, because cylinder 4 has the same size ring but a thicker skin than cylinder 2; relative to the surrounding structure, then, the ring in cylinder 4 is more flexible than that in cylinder 2. Again, for any given cylinder the maximum moment coefficient decreases as the load is moved closer to the root of the cylinder, because the region of the shell nearer the root is stiffer than the region farther away from the root, and a given ring is therefore relatively more flexible if it is located close to the root. The highest of all moment coefficients was therefore found on the tip ring of cylinder 3, which had the stiffest rings. The value of the experimental moment coefficient for this case was only 3 percent below the standard value of 0.239. This result indicates that the stresses in rings of practical proportions may approach quite closely the values predicted by the standard theory; however, the

bending stiffness of this ring is probably representative of main rather than secondary rings.

Figures 3 through 22 may be used to obtain quickly some idea of the stresses experienced by unloaded rings located near a loaded ring. The fact that such stresses exist is well known. Not so well known appears to be the necessary corollary that, if several adjacent rings are loaded simultaneously, the stress conditions in the center of the group approach the conditions assumed by the standard theory; that is, the ring bending stresses are higher and the skin shear stresses lower than they are when only one ring is loaded at a time. Some tests were made with loads applied simultaneously to three rings, and the stresses were found to agree within the experimental error with the stresses predicted by superposing the results obtained with individual load application.

Skin shear coefficients.- The skin shear coefficients C_q shown in figures 23 to 30 are defined by the equation

$$q = C_q \frac{P}{R} \tag{7}$$

The agreement between the experimental values and the curves calculated by Hoff's theory with six to twelve Fourier coefficients is again quite good except in the vicinity of the maximum, where the agreement is somewhat poorer than for the moment coefficients. A comparison of the maximum values of C_q is given in table 3. The experimental values of C_q given in this table were obtained by fairing a curve through the experimental points in the vicinity of the maximum, the curve computed by Hoff's method being used as an aid in fairing where necessary.

It may be noted from the figures and from table 3 that the standard theory is generally more seriously in error for the skin shear stresses than for the ring bending moments. On cylinder 3, for instance, which has the stiffest rings, the maximum bending moment measured was 97 percent of the value predicted by the standard theory; the maximum measured shear stress on this cylinder, however, was 155 percent of the value predicted by the standard theory. In cylinder 1 with the most flexible rings, the bending moment was 32 percent of the value predicted by the standard theory, while the maximum shear stress in the same cylinder was 533 percent of the value predicted by

the standard theory. A study of figures 23 to 30 also shows that the standard theory is very misleading in that the location of the maximum shear stress is given as 90° from the load, while it is actually located somewhere between 15 and 45° from the load.

CONCLUSIONS

From the comparisons presented of experimental data and calculated results, obtained by several methods, of the bending stresses in circular fuselage rings and of the shear stresses in the skin between the rings, the following conclusions are drawn:

1. The maximum bending moments in the rings are less and the maximum skin shears are more than those predicted by the standard theory which assumes, in effect, rigid rings. In the stiffest rings tested, the maximum bending stresses were 97 percent of those predicted by the standard theory; in the most flexible rings they were only 32 percent. Corresponding values for the shear stresses in the skin were 155 percent and 533 percent, respectively. The maximum shear stresses occur, very roughly, 30° from a radial load instead of 90° as predicted by the standard theory.

2. The method of Wignot, Combs, and Ensrud used in its original form may give large errors opposite in sign to those of the standard method.

3. The method of Hoff, extended where necessary, gives satisfactory agreement with the test results in most cases.

4. The method of Wignot, Combs, and Ensrud modified by redefining the "relative stiffness parameter" used by these authors gives somewhat less accuracy than Hoff's method but offers a considerable saving in time by the use of graphs.

Attention is called to the fact that the stress conditions resulting when a number of adjacent rings are loaded in a similar manner approach those defined by the standard theory.

Langley Memorial Aeronautical Laboratory
National Advisory Committee for Aeronautics
Langley Field, Va.

APPENDIX

THEORETICAL FORMULAS

The good agreement obtained between the experimentally determined moments in a flexible skin-supported ring with a radial load and the theory developed by Hoff in reference 2 justified the extension of the theory to other types of loadings. Basically, only three types of load need be considered in order to construct any load distribution; namely, the concentrated radial force, the concentrated tangential force, and the concentrated moment. The solution for the stresses caused by the concentrated radial load can be obtained as a limiting case of the solution of reference 2 but is given herein for the sake of completeness and unity of presentation. New solutions are developed for the stresses caused by a tangential force as well as by a concentrated moment.

Basic Assumptions and Theory

The theory used herein defines the stress distribution in a circular cylinder stiffened in the circumferential direction by rings and in the longitudinal direction by stringers. The cylinder is cantilevered from a rigid support. It is assumed that the shear flow in each sheet bay between rings does not vary in the longitudinal direction but may vary in the circumferential direction. Whatever material in the cross section of the cylinder is capable of resisting bending of the cylinder as a cantilever beam is assumed spread around the cylinder in a fictitious stringer sheet of thickness t'. Each reinforcing ring is of constant moment of inertia I and is capable of resisting only forces in its own plane. The notation used in numbering the sheet bays and rings and the positive directions of forces, moments, and stresses are given in figure 31.

On the basis of the assumptions made the shear flow q in the i^{th} bay can, for any loading, be expressed as

$$q_i = q_R + \sum_{2}^{\infty} a_{in} \sin n\varphi + \sum_{2}^{\infty} b_{in} \cos n\varphi \qquad (A1)$$

in which q_R represents the shear flow that is usually calculated on the basis of rigid rings and the two trigonometric series represent statically self-balancing shear flows. These self-balancing shear flows are also consistent with a self-balancing set of normal stresses in the stringer sheet. Only the sine series occurs if a symmetrical load is applied and only the cosine series occurs if the loading is antisymmetrical. The coefficients a_{in} and b_{in} are to be defined by a minimum of strain energy of the entire structure.

The moments, shear forces, and tangential forces in the reinforcing rings that are consistent with the shear flows in the sheet bays adjacent to rings and that also satisfy the conditions of continuity of the rings are:

$$M_i = M_R + R^2 \sum_{2}^{\infty} \frac{a_{in} - a_{(i-1)n}}{n(n^2 - 1)} \cos n\varphi - R^2 \sum_{2}^{\infty} \frac{b_{in} - b_{(i-1)n}}{n(n^2 - 1)} \sin n\varphi \tag{A2}$$

$$V_i = V_R - R \sum_{2}^{\infty} \frac{a_{in} - a_{(i-1)n}}{(n^2 - 1)} \sin n\varphi - R \sum_{2}^{\infty} \frac{b_{in} - b_{(i-1)n}}{(n^2 - 1)} \cos n\varphi \tag{A3}$$

$$H_i = H_R + R \sum_{2}^{\infty} \frac{n(a_{in} - a_{(i-1)n})}{(n^2 - 1)} \cos n\varphi - R \sum_{2}^{\infty} \frac{n(b_{in} - b_{(i-1)n})}{(n^2 - 1)} \sin n\varphi \tag{A4}$$

The stringer sheet stresses can be obtained from the shear flows and, because these stresses vary linearly along any cylindrical element, need only be defined at

the rings. If the stresses at the first ring are assumed to be zero, the stringer sheet stresses at the i^{th} ring are

$$\sigma_i = \sigma_R + \frac{1}{Rt'}\sum_{2}^{\infty}\left(a_{1n}L_1 + a_{2n}L_2 + \cdots a_{(i-1)n}L_{(i-1)}\right)\cos n\varphi$$

$$- \frac{1}{Rt'}\sum_{2}^{\infty}\left(b_{1n}L_1 + b_{2n}L_2 + \cdots b_{(i-1)n}L_{(i-1)}\right)\sin n\varphi \qquad (A5)$$

where σ_R is the stress given by the simple engineering theory of the bending of the cylinder.

If the total strain energy of the structure is minimized with respect to the coefficients of the terms of the series, sets of simultaneous equations will be obtained for the coefficients. (See reference 2.) A set of simultaneous equations will result for each value of n for the coefficient a_{in} and a separate set for each value of n for the coefficient b_{in}. Each set of equations will contain as many equations as there are bays.

Concentrated Radial Force

If a radial force P is applied to any ring of the cylinder at the location $\varphi = 0^{\circ}$, the shear flow q in the i^{th} bay, when the i^{th} bay is between the loaded ring and the root, is

$$q_i = -\frac{P}{\pi R}\sin\varphi + \sum_{2}^{\infty} a_{in}\sin n\varphi \qquad (A6)$$

and, when the i^{th} bay is between the tip and the loaded ring, is simply

$$q_i = \sum_{2}^{\infty} a_{in}\sin n\varphi \qquad (A6a)$$

The moments, shear forces, and tangential forces in the loaded ring are

$$M_i = \frac{PR}{2\pi}\left[1 + \frac{\cos\varphi}{2} - (\pi - \varphi)\sin\varphi\right] + R^2\sum_{2}^{\infty}\frac{a_{in} - a_{(i-1)n}}{n(n^2 - 1)}\cos n\varphi \quad (A7)$$

$$V_i = \frac{P}{2\pi}\left[\frac{\sin\varphi}{2} - (\pi - \varphi)\cos\varphi\right] - R\sum_{2}^{\infty}\frac{a_{in} - a_{(i-1)n}}{(n^2 - 1)}\sin n\varphi \quad (A8)$$

$$H_i = -\frac{P}{2\pi}\left[(\pi - \varphi)\sin\varphi + \frac{3}{2}\cos\varphi\right] + R\sum_{2}^{\infty}\frac{n\left(a_{in} - a_{(i-1)n}\right)}{(n^2 - 1)}\cos n\varphi \quad (A9)$$

and if the i^{th} ring is unloaded, only the series terms of the equations occur.

If the assumption is made that the cylinder is of constant cross-section and all rings have the same moment of inertia and are equally spaced, minimizing the strain energy in the structure results in a simple set of equations defining the coefficients a_{in}. For instance, if a cylinder with six rings and bays is loaded at the second ring, the second equation of the set of six equations is obtained by setting equal to zero the partial derivative of the total strain energy with respect to a_{2n}. This procedure yields

$$\frac{\partial U}{\partial a_{2n}} = (27n^2 - A\gamma)a_{1n} + (26n^2 + 2A\gamma + B)a_{2n}$$

$$+ (21n^2 - A\gamma)a_{3n} + 15n^2a_{4n} + 9n^2a_{5n} + 3n^2a_{6n} + \frac{PA\gamma n}{\pi R} = 0$$

The notation used is that of reference 2; that is

$$A = \frac{6R^6t'}{IL^3}$$

$$B = \frac{6Et'R^2}{GtL^2}$$

$$\gamma = \frac{1}{n^2\left(n^2 - 1\right)^2}$$

The general form of the six equations is given in table 4, but the load term $PA\gamma n/\pi R$ is placed on the right-hand side of the equation. The load term also occurs with a negative sign in the second equation and with a positive sign in the first equation. If the radial load had been applied in some ring other than ring 2, the load term would have appeared with the negative sign on the right-hand side of the equation having the same number as the loaded ring and with a positive sign on the right-hand side of the equation preceding it. Zeros would have appeared on the right-hand side of the other equations.

Concentrated Tangential Force

If a tangential force T is applied to any ring of the cylinder at the location $\varphi = 0^0$ the shear flow q in the i^{th} bay between the loaded ring and the root is

$$q_i = -\frac{T}{\pi R}\left(\frac{1}{2} + \cos\varphi\right) + \sum_{2}^{\infty} b_{in} \cos n\varphi \qquad ((A10)$$

and if the i^{th} bay is between the loaded ring and the tip the shear flow may be expressed as

$$q_i = \sum_{2}^{\infty} b_{in} \cos n\varphi \qquad (A10a)$$

If the i^{th} ring is loaded, the moments, shear forces and tangential forces are

$$M_i = \frac{TR}{2\pi}\left[(\pi - \varphi)(1 - \cos\varphi) - \frac{3}{2}\sin\varphi\right] - R^2\sum_{2}^{\infty}\frac{b_{in} - b_{(i-1)n}}{n(n^2 - 1)}\sin n\varphi \qquad (A11)$$

$$V_i = \frac{T}{2\pi}\left[(\pi - \varphi)\sin\varphi - \frac{\cos\varphi}{2} - 1\right] - R\sum_{2}^{\infty}\frac{b_{in} - b_{(i-1)n}}{n^2 - 1}\cos n\varphi \qquad (A12)$$

$$H_i = \frac{T}{2\pi}\left[\frac{\sin\varphi}{2} - (\pi - \varphi)\cos\varphi\right] - R\sum_{2}^{\infty}\frac{n\left(b_{in} - b_{(i-1)n}\right)}{n^2 - 1}\sin n\varphi \qquad (A13)$$

For the rings not loaded the moments are expressed only in terms of the series. If the assumption is again made that the cylinder has six bays and is of constant cross section and that the rings have equal stiffness and are equally spaced, the sets of equations defining the coefficients b_{in} are the same as those defining the coefficients a_{in} for the radial load, except that the value of the load term on the right-hand side of the equation is now $TA\varphi/\pi R$. The load term appears with the negative sign on the right-hand side of the equation having the same number as the loaded ring, and with the positive sign in the equation preceding it. Zeros occur in the right-hand side of all other equations.

Concentrated Moment

If a concentrated moment M_o is applied to any ring of the cylinder, at the location $\varphi = 0^\circ$, the shear flow in the i^{th} bay when the bay is between the loaded ring and the root is

$$q_i = -\frac{M_o}{2\pi R^2} + \sum_{2}^{\infty} b_{in} \cos n\varphi \qquad (A14)$$

and when the i^{th} bay is between the tip and the loaded ring the shear flow is

$$q_i = \sum_{2}^{\infty} b_{in} \cos n\varphi \qquad (A14a)$$

The moments, shear forces, and tangential forces in the loaded ring are

$$M_i = \frac{M_o}{2\pi}\left[(\pi - \varphi) - 2 \sin \varphi\right] - R^2 \sum_{2}^{\infty} \frac{b_{in} - b_{(i-1)n}}{n(n^2 - 1)} \sin n\varphi \qquad (A15)$$

$$V_i = -\frac{M_o}{2\pi R}(1 + 2 \cos \varphi) - R \sum_{2}^{\infty} \frac{b_{in} - b_{(i-1)n}}{n^2 - 1} \cos n\varphi \qquad (A16)$$

$$H_i = -\frac{M_o}{\pi R} \sin \varphi - R \sum_{2}^{\infty} \frac{n(b_{in} - b_{(i-1)n})}{n^2 - 1} \sin n\varphi \qquad (A17)$$

In the unloaded rings the moments and forces are given by the series expressions. If a cylinder of constant cross section stiffened by six equally spaced rings of constant moment of inertia is considered, the set of equations given in table 4 applies again except that the value of the load term is $\frac{M_o A_\gamma}{\pi R^2}(n^2 - 1)$. The load term appears with the positive sign on the right-hand side of the equation having the same number as the loaded ring, and with the negative sign in the equation preceding it. Zeros occur on the right-hand side of all other equations.

Rules for Writing Equations

The left-hand side of the equations defining the coefficients a_{in} or b_{in} can be written for a cylinder of constant cross section having any number of bays between equally spaced rings of equal stiffness if the following features are observed in the scheme of equations in table 4. All the elements lying along the main diagonal that runs from the upper left to the lower right-hand corner contain the term $(2A_\gamma + B)$ except the one in the lower right-hand corner for which the coefficient of A_γ is unity. The elements to the left and right of the element on the main diagonal contain the term $-A_\gamma$. All the elements contain the term n^2, the coefficients of which follow a simple pattern. The coefficients of n^2 in the elements in the main diagonal start with 2 in the lower right-hand corner and increase by 6 in each element lying above and to the left. The coefficient of n^2 in any element in the column above an element on the main diagonal or in the row to the left is one more than the coefficient of n^2 in the element on the main diagonal.

The right-hand side of the equations can be easily written as follows: For the equation bearing the same number as the loaded ring and the equation preceding it, the appropriate load term is written down as shown in table 4. For all other equations, zeros are put down.

It can be shown that the scheme of writing the equations can also be used for the general loading case where any number of loads are acting on the ring. The load system is separated into a symmetrical and an

antisymmetrical part, and the rigid-ring bending moments caused by the entire load system are represented by the series

$$M_R = \sum_{2}^{\infty} C_n \sin n\varphi + \sum_{2}^{\infty} D_n \cos n\varphi$$

where the Fourier coefficients C_n define the antisymmetrical part and the coefficients D_n the symmetrical part of the moment. The load term appearing in the scheme of equations of table 4 is, then, for antisymmetrical loads

$$C_n \frac{A\nu n(n^2 - 1)}{R^2}$$

and for symmetrical loads,

$$D_n \frac{A\nu n(n^2 - 1)}{R^2}$$

For the antisymmetrical loads the sign of the load term on the right-hand side of the equation with the same number as the loaded ring is opposite to that of C_n; for symmetrical loads the sign of the load term for the same equation is the same as that of D_n.

Numerical Example

Basic data.- The numerical example chosen is test cylinder 3 with a radial load applied at ring 3. The basic data are therefore (from table 1):

Radius, R, inches	15
Spacing of rings, L, inches	15
Thickness, $t = t'$, inch	0.0320
Moment of inertia, I, inches^4	0.357

The value of G/E is taken as 0.377. With these numerical values, the constants A and B appearing in table 4 become:

$$A = 1815.4$$

$$B = 15.90$$

Determination of Fourier coefficients.- Because cylinder 3 has rather stiff rings, a few Fourier coefficients give sufficient accuracy. For this numerical example, the coefficients for $n = 2$, 3, and 4 will be determined.

The cylinder has four bays, whereas table 4 is set up for six bays. The left-hand sides of the equations are therefore obtained directly from table 4 by dropping the excess terms and retaining only the four rows and four columns appropriate to a four-bay cylinder, starting in the lower right-hand corner of the terms on the left-hand side; that is, the first two columns and the two top rows in table 4 are dropped, and the remaining four columns and rows are renumbered from 1 to 4. The right-hand sides of the equations are obtained by putting the load terms in the places appropriate to the position of the load. The final general scheme for an arbitrary value of n is then:

$$(20n^2 + 2A\gamma + B)a_{1n} + (15n^2 - A\gamma)a_{2n} + 9n^2a_{3n} + 3n^2a_{4n} = 0$$

$$(15n^2 - A\gamma)a_{1n} + (14n^2 + 2A\gamma + B)a_{2n} + (9n^2 - A\gamma)a_{3n} + 3n^2a_{4n} = \frac{PA\gamma n}{\pi R}$$

$$9n^2a_{1n} + (9n^2 - A\gamma)a_{2n} + (8n^2 + 2A\gamma + B)a_{3n} + (3n^2 - A\gamma)a_{4n} = -\frac{PA\gamma n}{\pi R}$$

$$3n^2a_{1n} + 3n^2a_{2n} + (3n^2 - A\gamma)a_{3n} + (2n^2 + A\gamma + B)a_{4n} = 0$$

The set of equations for determining the Fourier coefficients $n = 2$ is then obtained from this general scheme by setting $n = 2$ and inserting the numerical values for A, B, and γ. The sets of equations for determining the Fourier coefficients $n = 3$ and $n = 4$ are then obtained in an analogous manner. The three sets of simultaneous equations are solved by any suitable method, for instance, the Crout method (reference 4), and the resulting Fourier coefficients are

n	a_{1n}	a_{2n}	a_{3n}	a_{4n}
2	-0.04820P/R	-0.17368P/R	0.25394P/R	0.16711P/R
3	.02036P/R	-.08048P/R	.08348P/R	-.00992P/R
4	.00622P/R	-.01899P/R	.01902P/R	-.00601P/R

Determination of moment and shear coefficients.- The moment coefficient C_M is defined by

$$C_M = \frac{M}{PR}$$

By the use of the expression (A7) the moment coefficient for ring i can be written as

$$C_M = C_{M_R} + \frac{R}{P}\sum_{2}^{\infty} \frac{a_{in} - a_{(i-1)n}}{n(n^2 - 1)} \cos n\varphi$$

The coefficient for the moment at the point of application of the load ($\varphi = 0$, $i = 3$), for instance, becomes

$$C_M = C_{M_R} + \frac{R}{P}\sum_{2}^{\infty} \frac{a_{3n} - a_{2n}}{n(n^2 - 1)} \cos n\varphi$$

or, when terms after $n = 4$ are neglected,

$$C_M = -0.2387 + \frac{(0.2539 + 0.1737)}{6} \cos 2(0^\circ)$$

$$+ \frac{(0.0835 + 0.0805)}{24} \cos 3(0^\circ) + \frac{(0.0190 + 0.0190)}{60} \cos 4(0^\circ)$$

$$= -0.1600$$

The shear coefficient C_q is defined by

$$C_q = q\frac{R}{P}$$

By the use of expression (A1) the coefficient for bay i can be written as

$$C_q = C_{q_R} + \frac{R}{P}\sum_{2}^{\infty} a_{in} \sin n\varphi$$

where the second subscript R again denotes the value for the rigid ring. The shear stress reaches its maximum value in bay 3 ($i = 3$) at about $\varphi = 44^\circ$. The maximum shear coefficient is therefore given by

$$C_q = C_{q_R} + \frac{R}{P}\sum_{2}^{\infty} a_{3n} \sin n\varphi$$

or, numerically, if terms beyond $n = 4$ are dropped

$$C_q = 0.2211 + 0.2539 \sin 2(44^\circ) + 0.0834 \sin 3(44^\circ) + 0.0190 \sin 4(44^\circ)$$

$$= 0.5383$$

REFERENCES

1. Wise, Joseph A.: Analysis of Circular Rings for Monocoque Fuselages. Jour. Aero. Sci., vol. 6, no. 11, Sept. 1939, pp. 460-463.

2. Hoff, N. J.: Stresses in a Reinforced Monocoque Cylinder Under Concentrated Symmetric Transverse Loads. Jour. Appl. Mech., vol. 11, no. 4, Dec. 1944, pp. A-235 - A-239.

3. Wignot, J. E., Combs, Henry, and Ensrud, A. F.: Analysis of Circular Shell-Supported Frames. NACA TN No. 929, 1944.

4. Crout, Prescott D.: A Short Method for Evaluating Determinants and Solving Systems of Linear Equations with Real or Complex Coefficients. Supp. to Elec. Eng., Trans. Section, AIEE, vol. 60, Dec. 1941, pp. 1235-1240. (Abridged as Marchant Methods MM-182, Sept. 1941, Marchant Calculating Machine Co., Oakland, Calif.)

TABLE 1.- DIMENSIONS OF TEST CYLINDERS

Cylinder	Radius of cylinder R (in.)	Length of cylinder (in.)	Spacing of rings L (in.)	Thickness of skin t (in.)	Moment of inertia of ring, I ($in.^4$)
1	15	60	15	0.0322	0.00421
1a	15	60	30	.0322	.00421
1b	15	30	30	.0322	.00421
1c	15	15	15	.0322	.00424
2	15	60	15	.0320	.04001
3	15	60	15	.0320	.35695
4	15	60	15	.0648	.04526
4a	15	45	15	.0648	.04526

NATIONAL ADVISORY
COMMITTEE FOR AERONAUTICS

TABLE 2.- COMPARISONS OF THEORETICAL AND EXPERIMENTAL MAXIMUM BENDING MOMENT COEFFICIENTS

		(1)	(2)		(3)		(4)	(5)				
Cylinder	Loaded ring	C_M Experimental	C_M Computed according to reference 2	d Computed according to reference 3	C_M Computed according to reference 3	d Computed according to reference 3 (modified)	C_M Computed according to reference 3 (modified)	C_M Computed according to standard method	(2)/(1)	(3)/(1)	(4)/(1)	(5)/(1)
Radial load												
1	1	0.123	0.124	10,820	0.071	384.4	0.124	0.239	1.01	0.58	1.01	1.94
	2	.092	.095	10,820	.071	820.8	.109		1.03	.77	1.18	2.60
	3	.083	.086	10,820	.071	2156	.092		1.04	.86	1.11	2.88
	4	.074	.076	10,820	.071	7858	.075		1.03	.96	1.01	3.23
1a	1	.128	.137	10,820	.071	384.4	.124		1.07	.55	.97	1.87
1b	1	.106	.108	10,820	.071	2156	.092		1.02	.67	.87	2.25
1c	1	.082	.086	10,820	.071	7858	.075		1.05	.87	.91	2.91
2	1	.203	.172	1,132	.103	40.2	.181		.85	.51	.89	1.18
	2	.166	.133	1,132	.103	85.8	.157		.80	.62	.95	1.44
	3	.139	.118	1,132	.103	225.5	.135		.85	.74	.97	1.72
	4	.129	.104	1,132	.103	821.9	.109		.81	.80	.84	1.85
3	1	.233	.207	126.9	.147	4.51	.226		.89	.63	.97	1.03
	2	.198	.167	126.9	.147	9.62	.216		.84	.74	1.09	1.21
	3	.183	.160	126.9	.147	25.3	.195		.87	.80	1.07	1.31
	4	.170	.147	126.9	.147	92.1	.155		.86	.86	.91	1.41
4	1	.179	.159	2,026	.093	72.0	.163		.89	.52	.91	1.34
	2	.143	.121	2,026	.093	153.6	.143		.85	.65	1.00	1.67
	3	.132	.109	2,026	.093	403.6	.123		.83	.70	.93	1.81
	4	.122	.097	2,026	.093	1471	.098		.80	.76	.80	1.96
Tangential load												
4a	1	0.031	0.027	2,026	0.011	153.6	0.027	0.064	0.87	0.36	0.87	2.06

NATIONAL ADVISORY
COMMITTEE FOR AERONAUTICS

TABLE 3.- COMPARISONS BETWEEN THEORETICAL AND EXPERIMENTAL MAXIMUM SHEAR FLOW COEFFICIENTS FOR RADIAL LOAD

			(1)	(2)	(3)	(4)	(5)				
Cylinder	Loaded ring	Measured bay	C_q Experimental	C_q Computed according to reference 2	C_q Computed according to reference 3	C_q Computed according to reference 3 (modified)	C_q Computed according to standard method	(2)/(1)	(3)/(1)	(4)/(1)	(5)/(1)
1	1	1	1.24	1.23	3.36	1.15	0.31	0.99	2.71	0.93	0.25
	1	3	.81	.83	3.36	1.15		1.02	4.15	1.42	.38
	3	2	.94	.87	1.63	.92		.93	1.73	.98	.33
	3	3	1.65	1.57	1.73	1.05		.95	1.05	.64	.19
2	1	1	.78	.70	1.60	.60		.90	2.05	.77	.40
	1	3	.37	.42	1.60	.60		1.14	4.32	1.62	.84
	3	2	.55	.47	.72	.41		.85	1.31	.75	.56
	3	3	1.07	.92	.88	.59		.86	.82	.55	.29
3	1	1	.48	.43	.85	.36		.90	1.77	.75	.65
	1	3	.32	.34	.85	.36		1.06	2.66	1.12	.97
	3	2	.27	.25	.32	.16		.93	1.19	.59	1.15
	3	3	.51	.53	.52	.37		1.04	1.02	.73	.61
4	1	1	.90	.80	1.95	.70		.89	2.17	.78	.34
	1	3	.48	.50	1.95	.70		1.04	4.06	1.46	.65
	3	2	.69	.55	.91	.49		.80	1.32	.71	.45
	3	3	1.13	1.07	1.04	.62		.95	.92	.55	.27

NATIONAL ADVISORY
COMMITTEE FOR AERONAUTICS

TABLE 4.- SCHEME OF EQUATIONS FOR CYLINDER OF SIX EQUAL BAYS LOADED AT SECOND RING

$$\left[A = \frac{6R^6t'}{IL^3};\ B = \frac{6Et'R^2}{GtL^2};\ \gamma = \frac{1}{n^2(n^2-1)^2}\right]$$

Coefficients (1) / Equation number	Left-hand side						Right-hand side (Load term)		
	a_{1n}	a_{2n}	a_{3n}	a_{4n}	a_{5n}	a_{6n}			
	b_{1n}	b_{2n}	b_{3n}	b_{4n}	b_{5n}	b_{6n}	Radial	Tangential	Moment
1	$32n^2 + 2A\gamma + B$	$27n^2 - A\gamma$	$21n^2$	$15n^2$	$9n^2$	$3n^2$	$PA\gamma n/\pi R$	$TA\gamma/\pi R$	$-M_oA\gamma(n^2-1)/\pi R^2$
2	$27n^2 - A\gamma$	$26n^2 + 2A\gamma + B$	$21n^2 - A\gamma$	$15n^2$	$9n^2$	$3n^2$	$-PA\gamma n/\pi R$	$-TA\gamma/\pi R$	$M_oA\gamma(n^2-1)/\pi R^2$
3	$21n^2$	$21n^2 - A\gamma$	$20n^2 + 2A\gamma + B$	$15n^2 - A\gamma$	$9n^2$	$3n^2$	0	0	0
4	$15n^2$	$15n^2$	$15n^2 - A\gamma$	$14n^2 + 2A\gamma + B$	$9n^2 - A\gamma$	$3n^2$	0	0	0
5	$9n^2$	$9n^2$	$9n^2$	$9n^2 - A\gamma$	$8n^2 + 2A\gamma + B$	$3n^2 - A\gamma$	0	0	0
6	$3n^2$	$3n^2$	$3n^2$	$3n^2$	$3n^2 - A\gamma$	$2n^2 + A\gamma + B$	0	0	0

[1]Coefficients a apply to radial load; coefficients b to tangential or moment load.

NATIONAL ADVISORY
COMMITTEE FOR AERONAUTICS

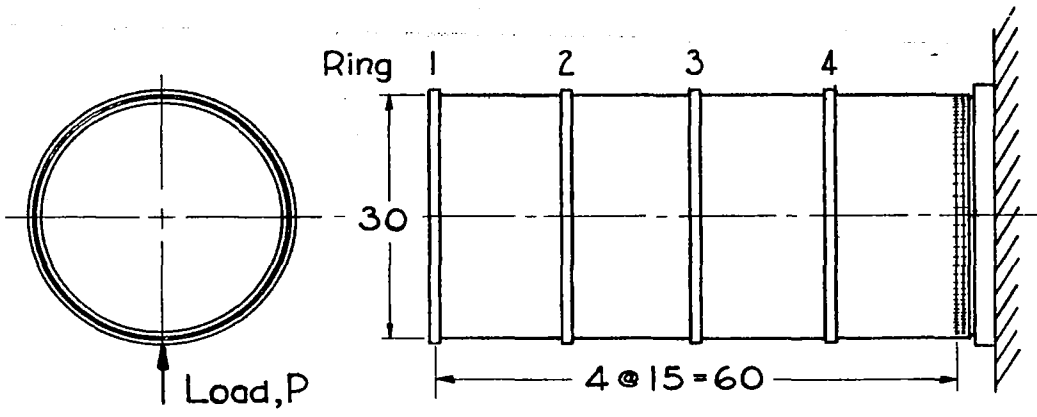

NATIONAL ADVISORY COMMITTEE FOR AERONAUTICS

Figure 1. – General over-all cylinder dimensions.

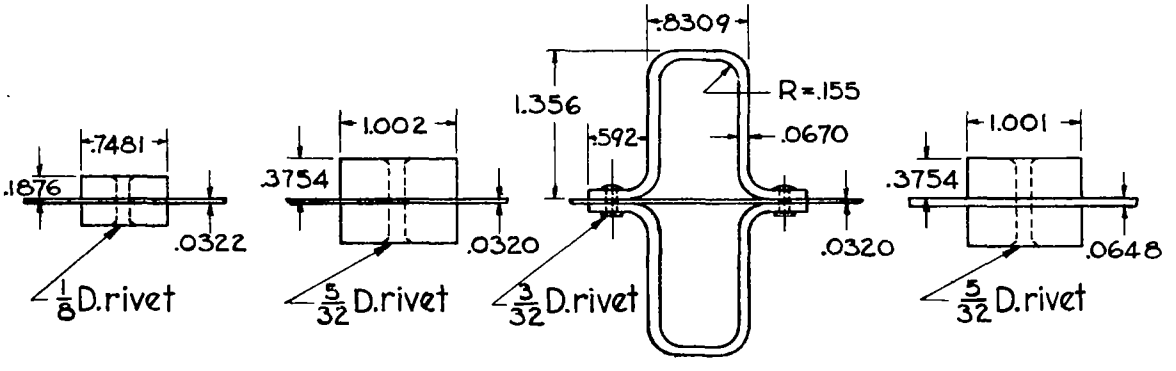

NATIONAL ADVISORY COMMITTEE FOR AERONAUTICS

Figure 2. – Dimensions of rings and rivet sizes for various cylinders. Rivet spacing, 1 inch.

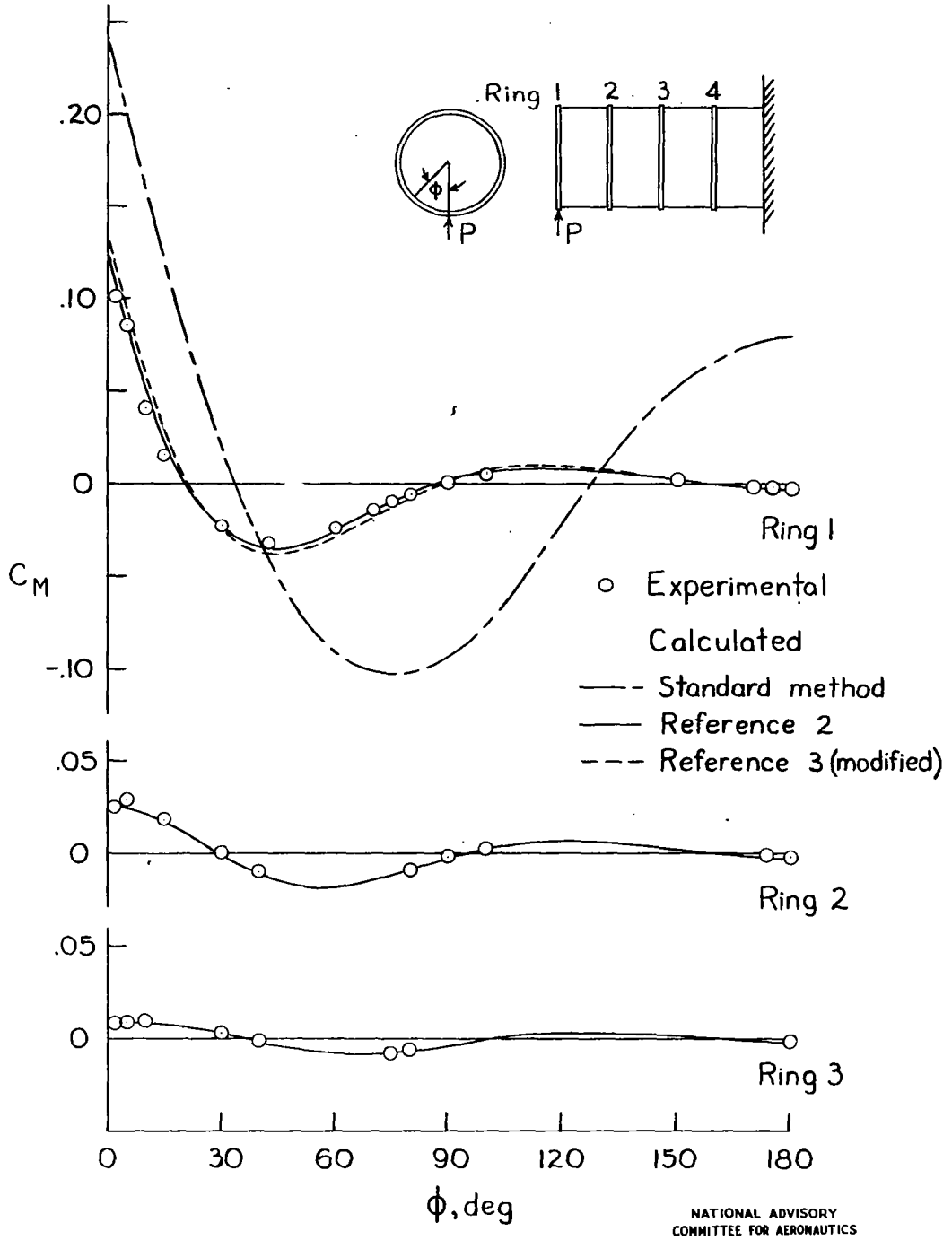

Figure 3. - Ring bending-moment coefficients in cylinder 1 for radial load at ring 1.

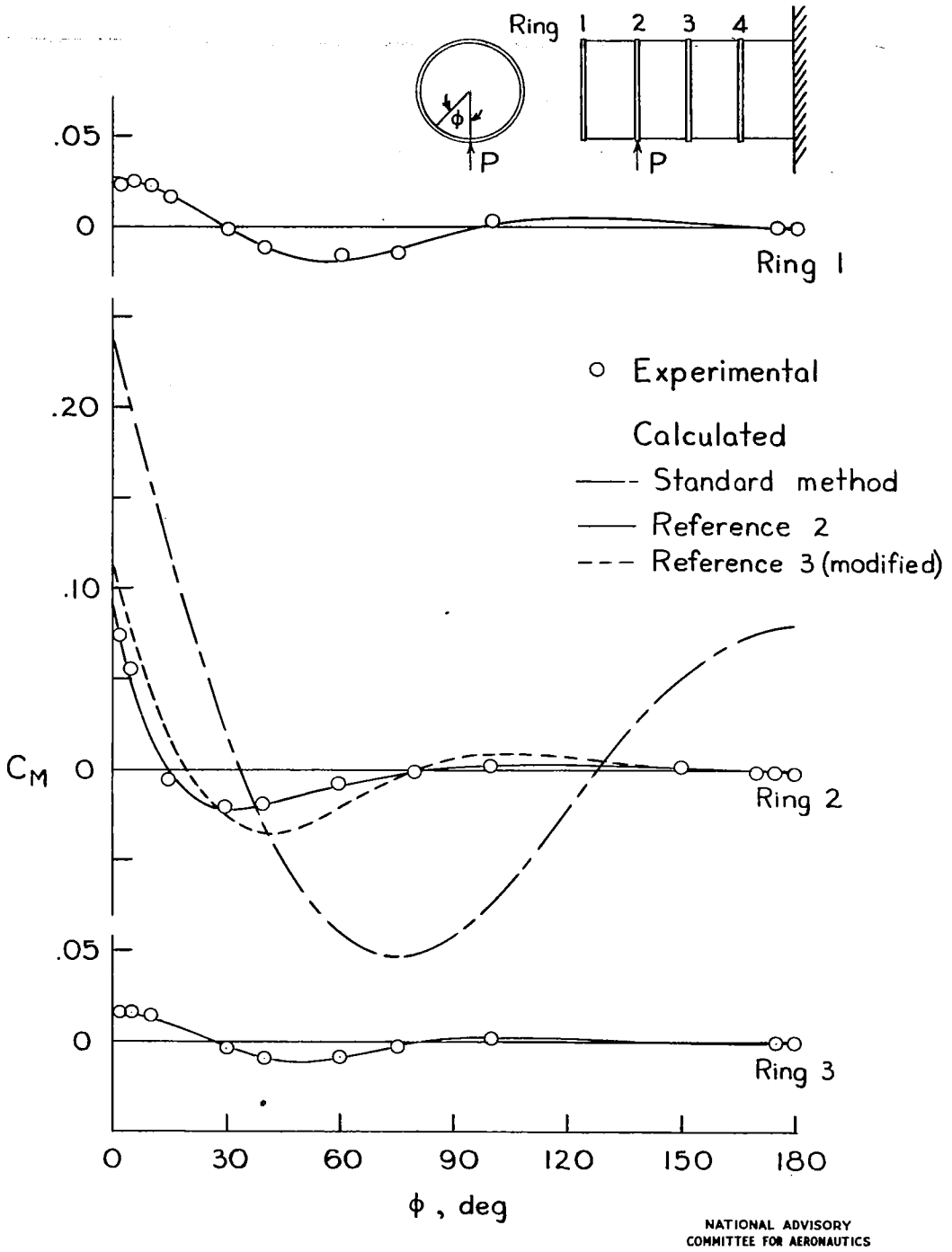

Figure 4.- Ring bending-moment coefficients in cylinder 1 for radial load at ring 2.

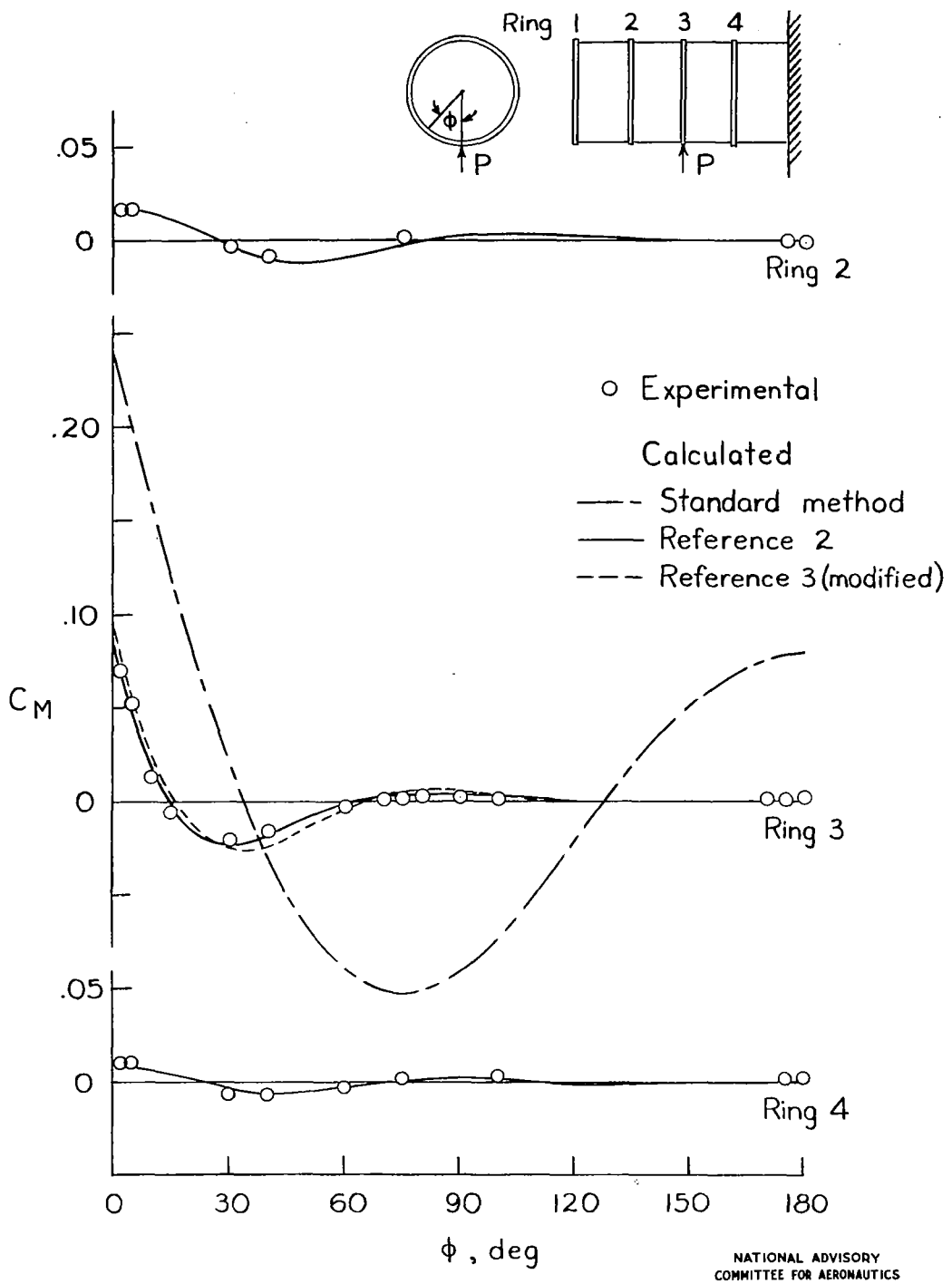

Figure 5.- Ring bending-moment coefficients in cylinder 1 for radial load at ring 3.

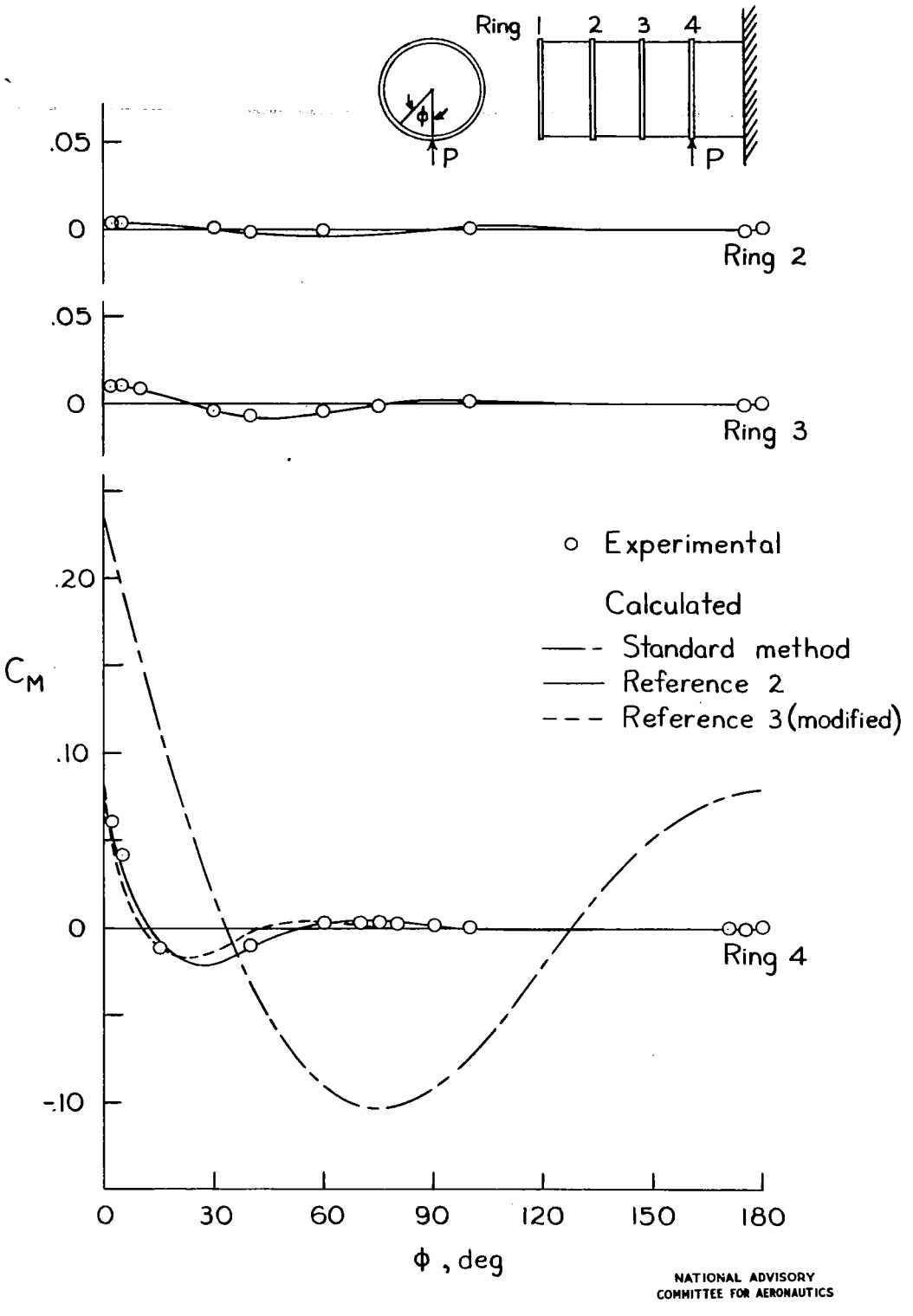

Figure 6.- Ring bending-moment coefficients in cylinder 1 for radial load at ring 4.

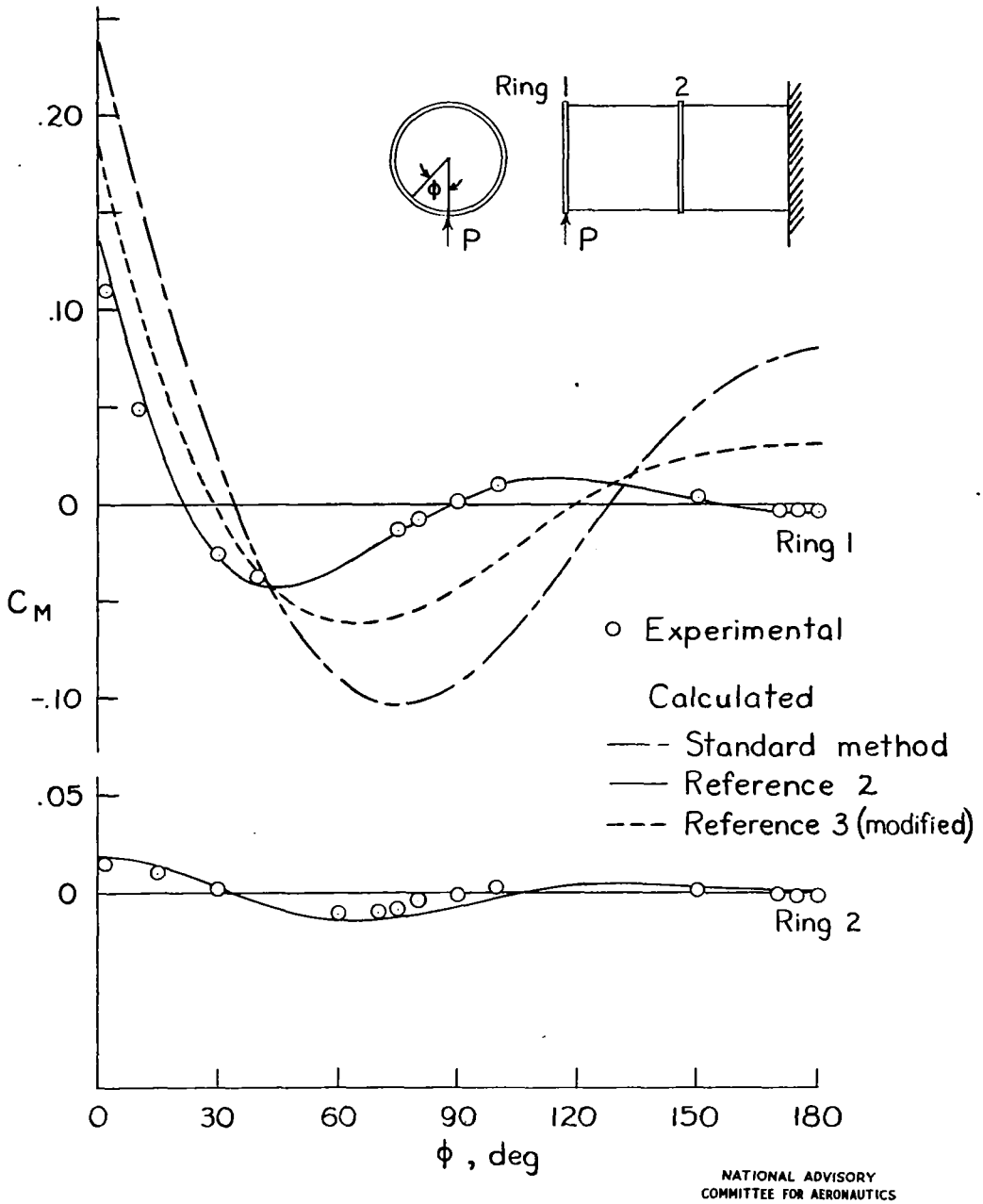

Figure 7.- Ring bending-moment coefficients in cylinder 1a for radial load at ring 1.

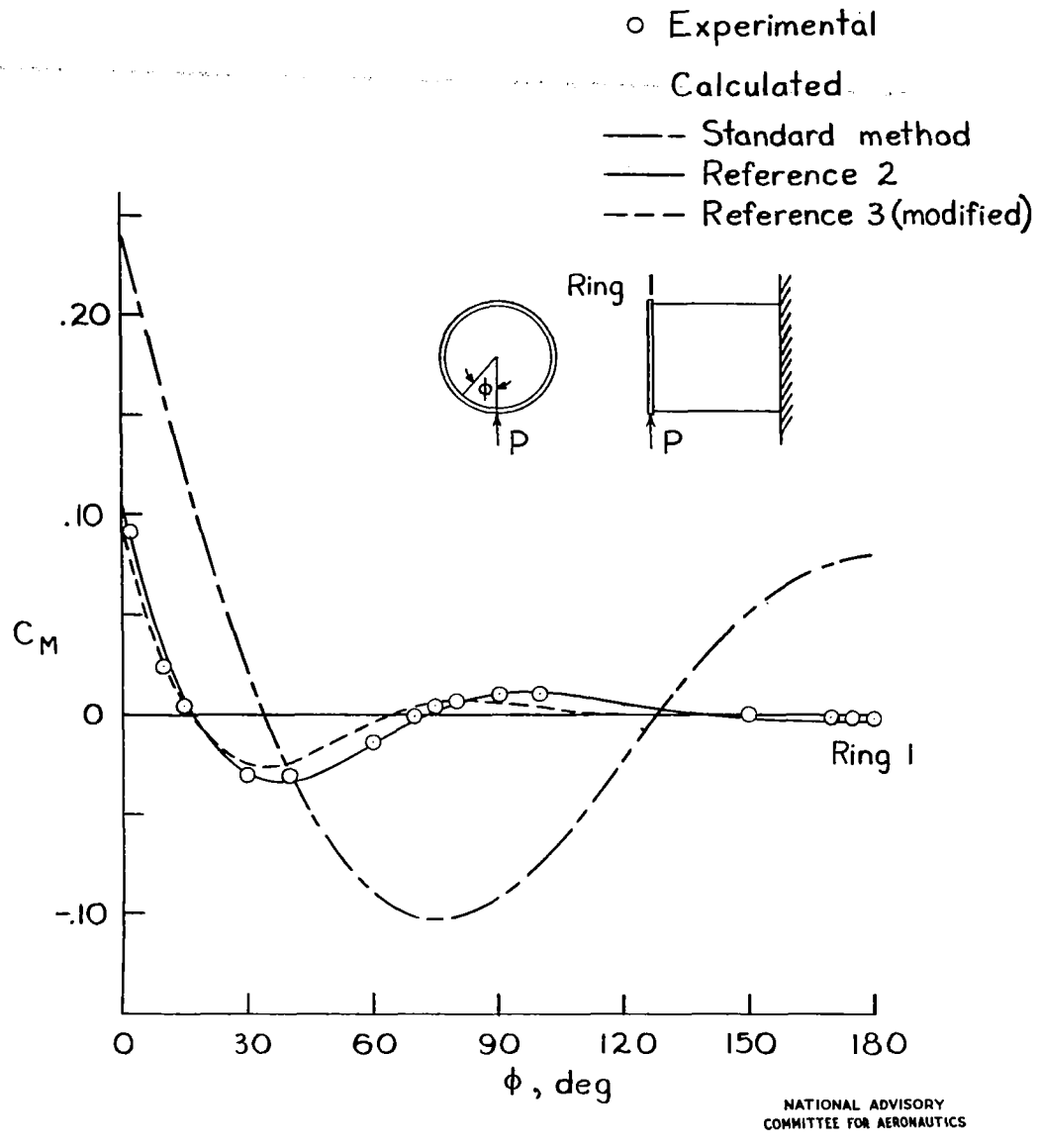

Figure 8. – Ring bending-moment coefficients in cylinder 1b for radial load at ring 1.

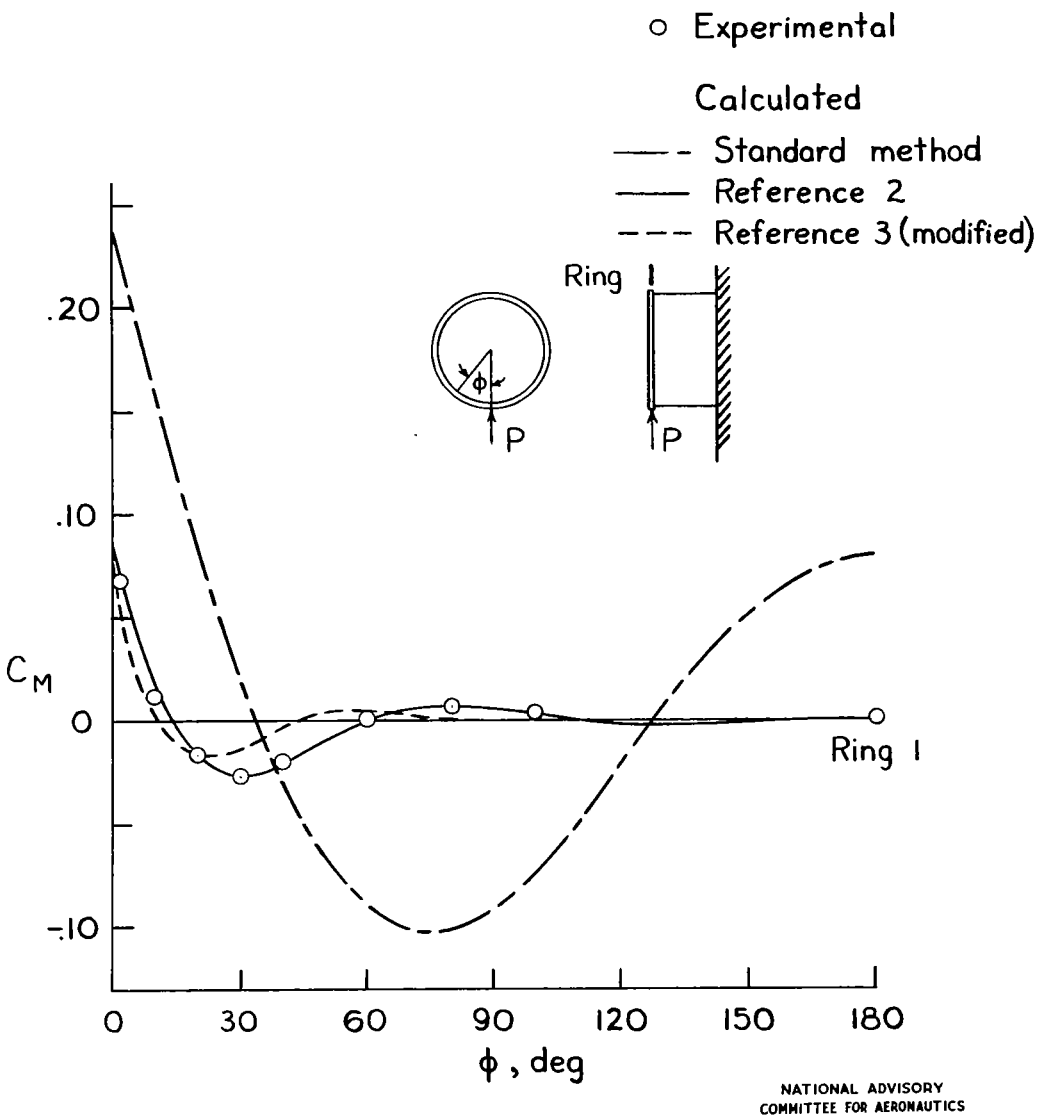

Figure 9. - Ring bending - moment coefficients in cylinder Ic for radial load at ring 1.

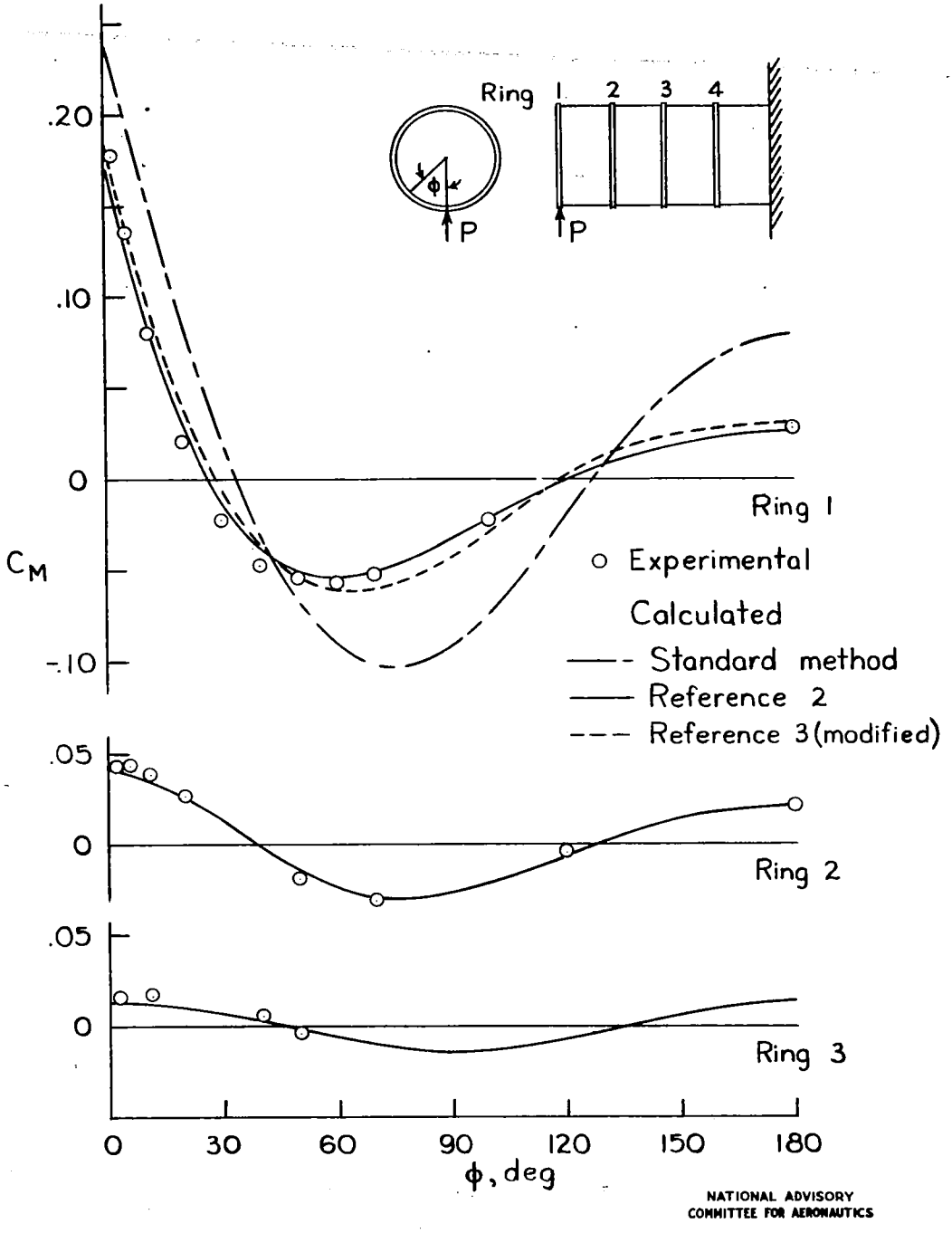

Figure 10.- Ring bending-moment coefficients in cylinder 2 for radial load at ring 1.

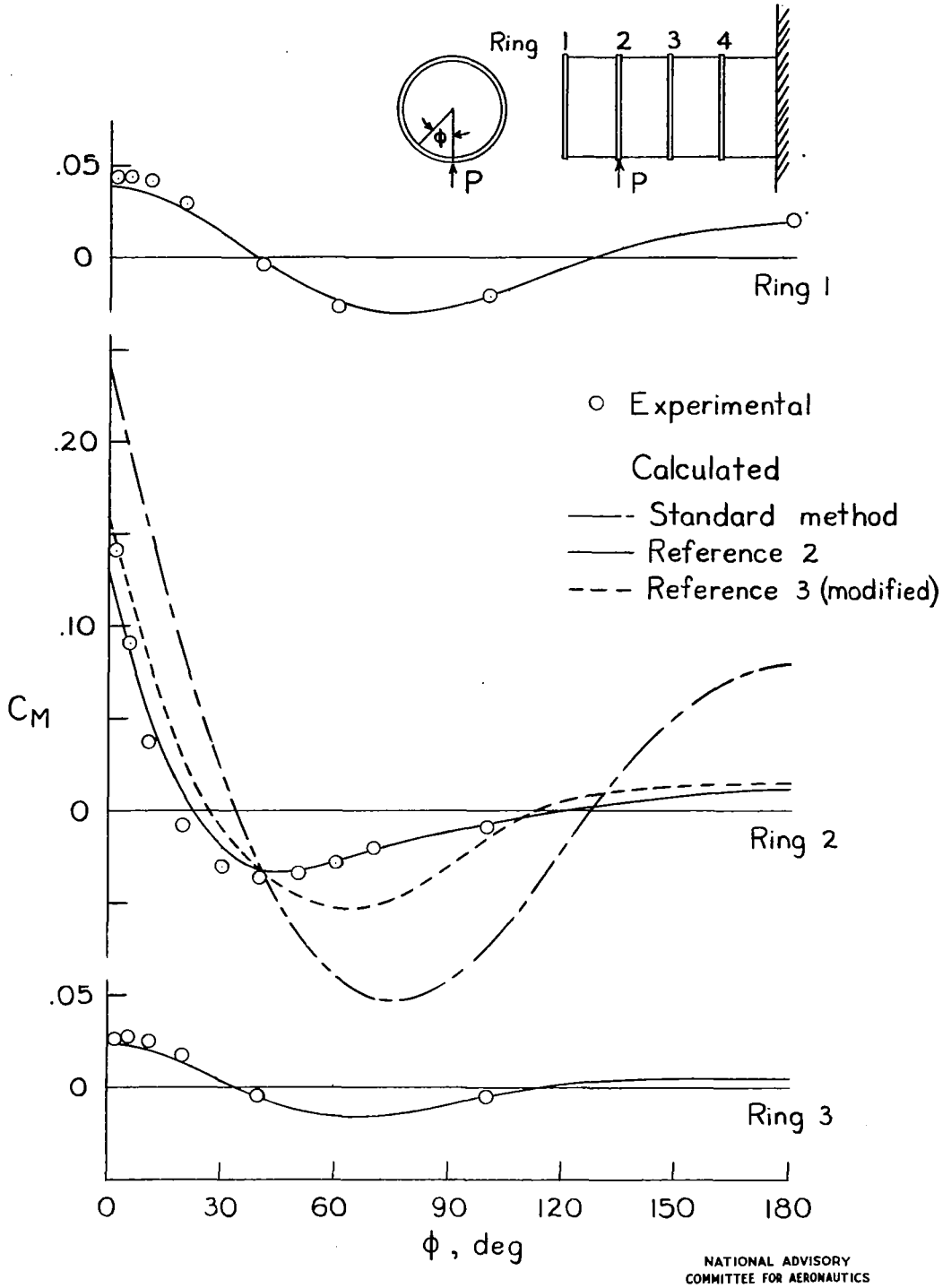

Figure 11.- Ring bending-moment coefficients in cylinder 2 for radial load at ring 2.

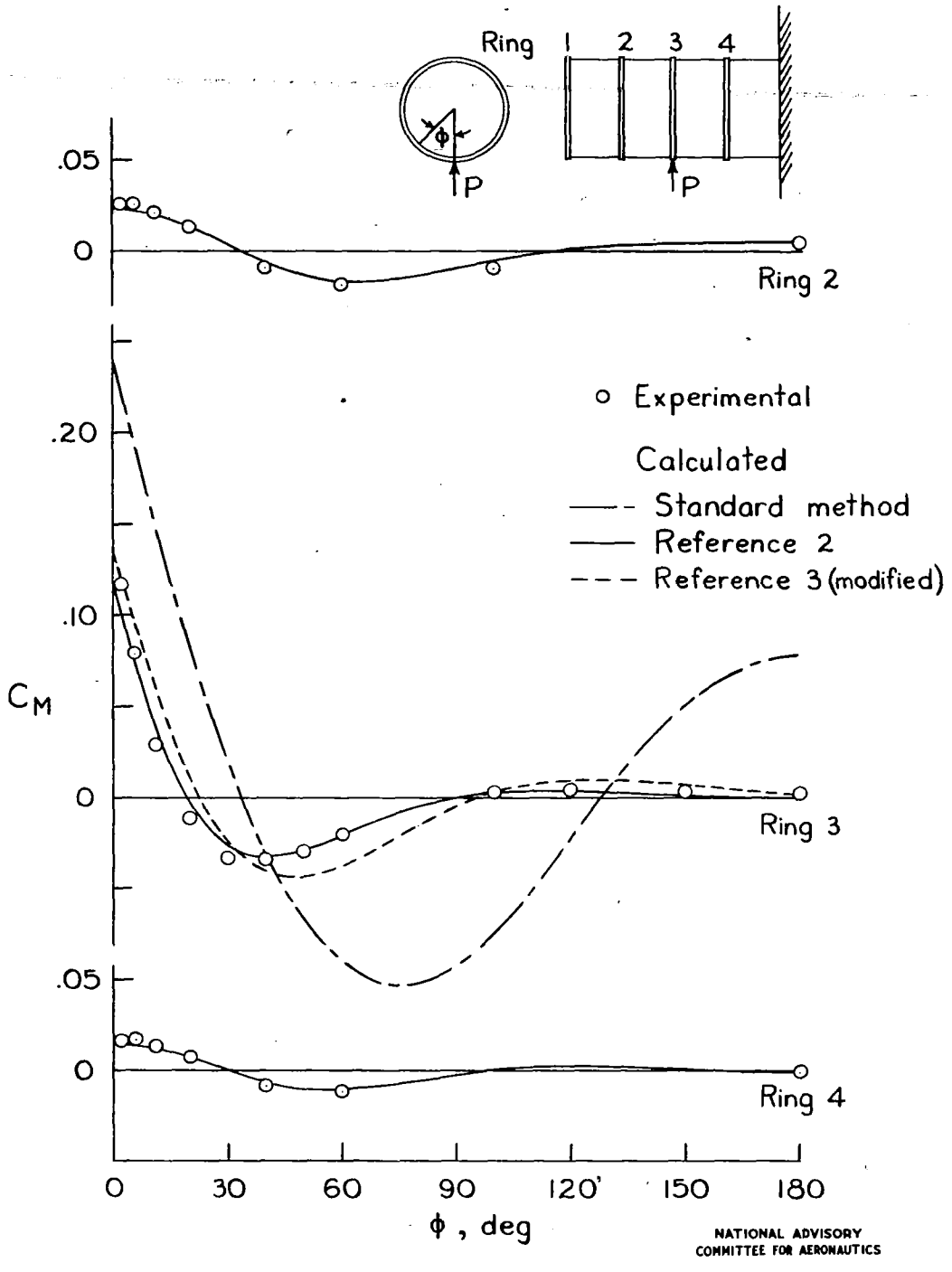

Figure 12.- Ring bending-moment coefficients in cylinder 2 for radial load at ring 3.

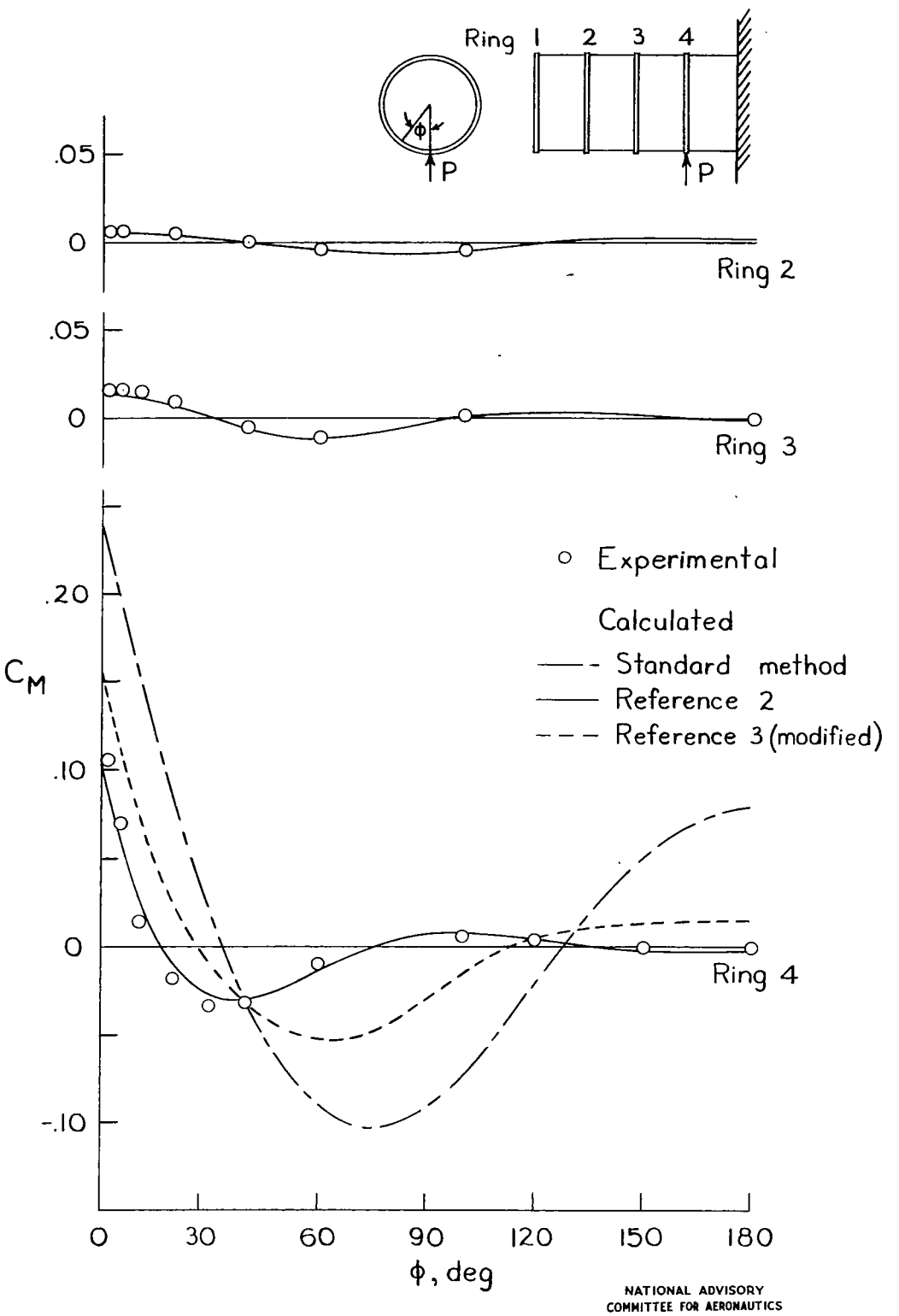

Figure 13. – Ring bending-moment coefficients in cylinder 2 for radial load at ring 4.

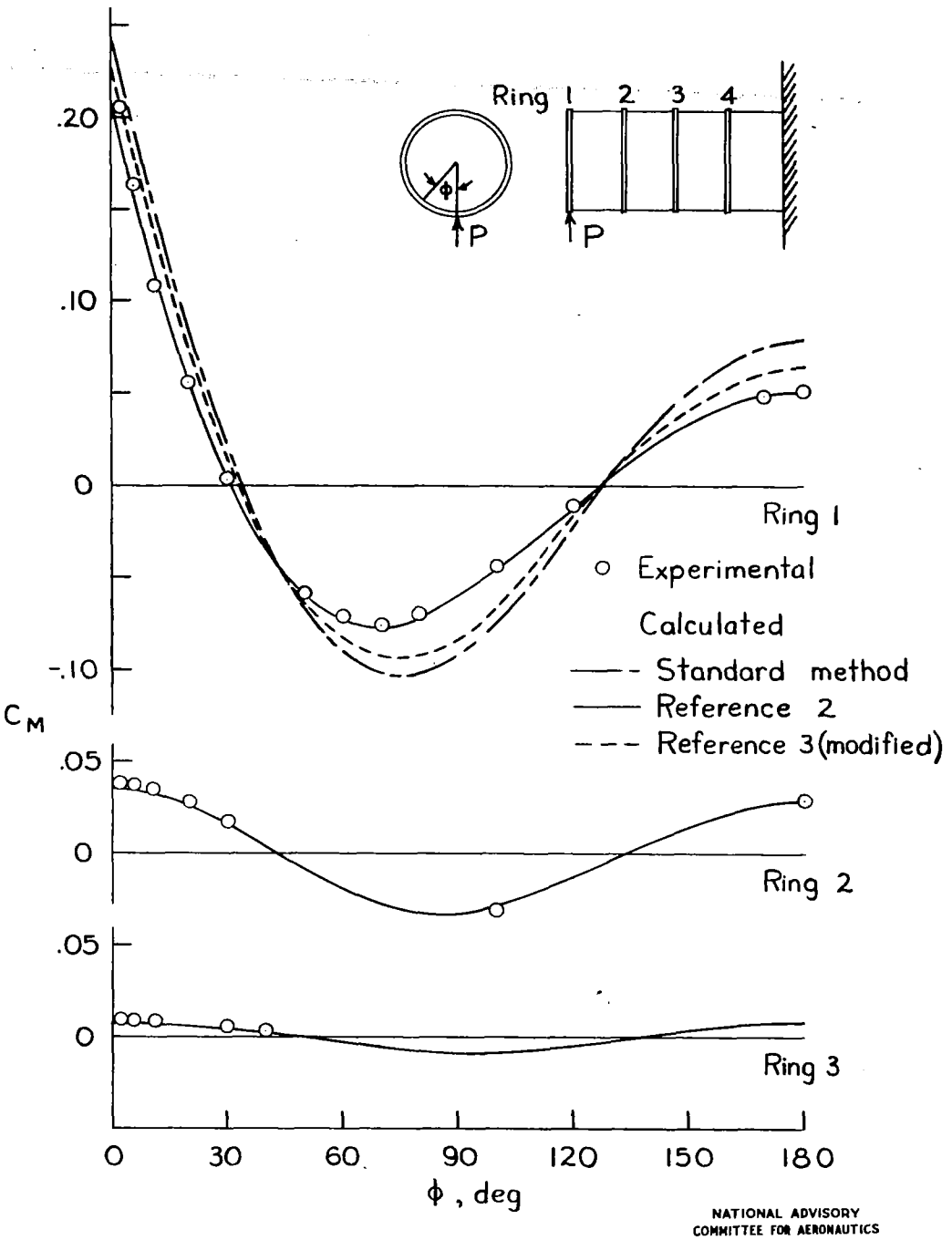

Figure 14. - Ring bending - moment coefficients in cylinder 3 for radial load at ring 1.

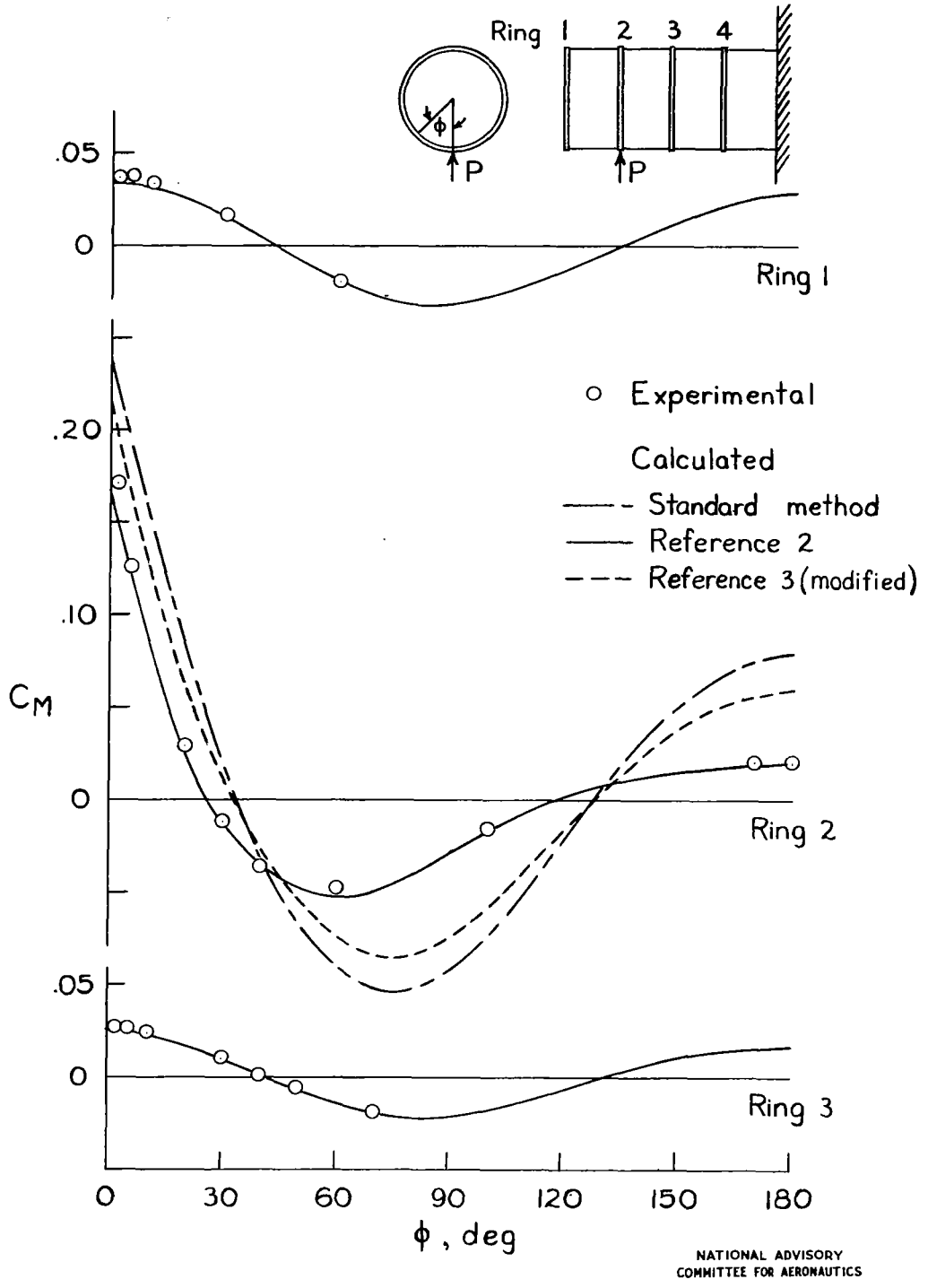

Figure 15. - Ring bending-moment coefficients in cylinder 3 for radial load at ring 2.

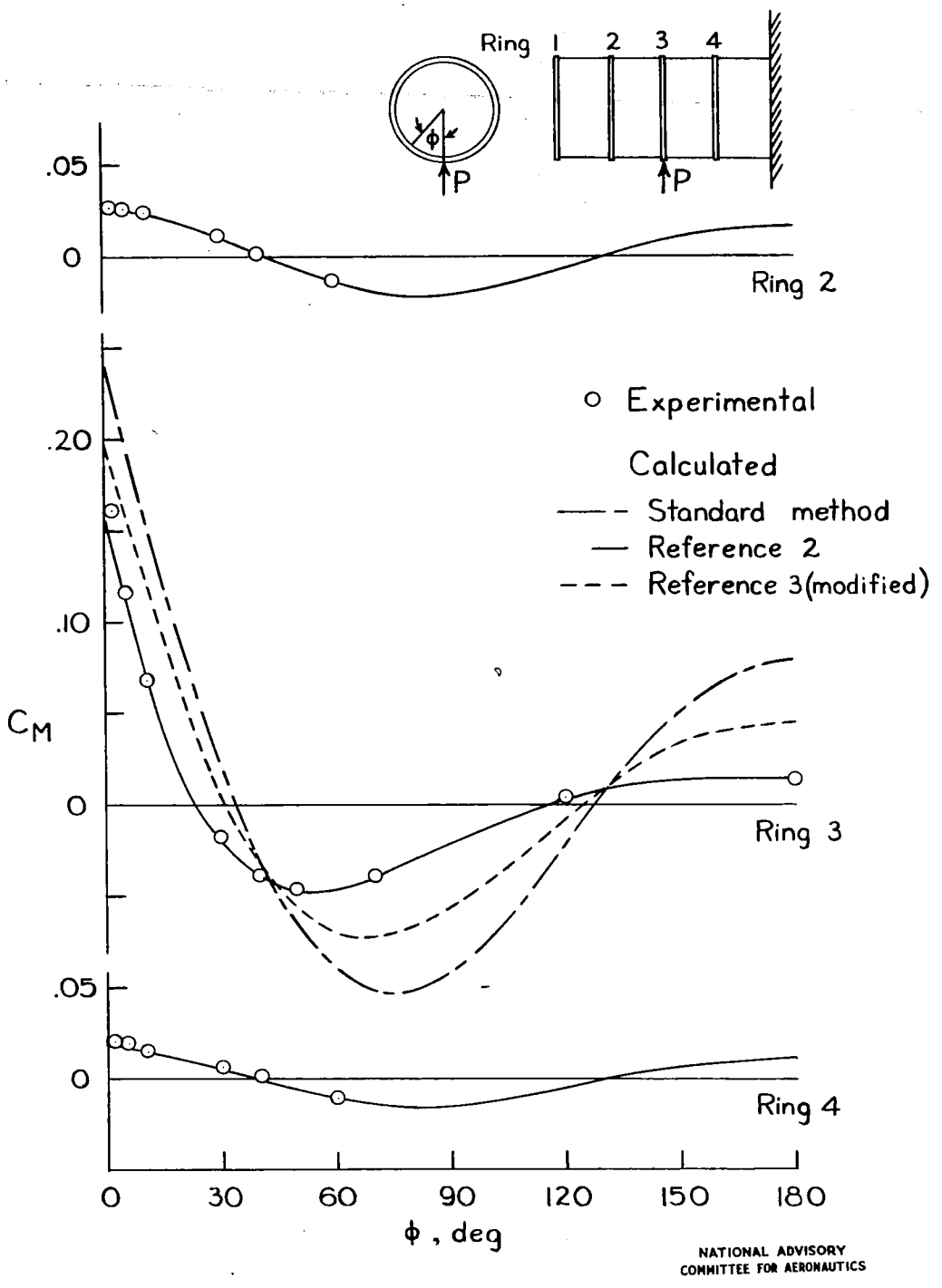

Figure 16.- Ring bending-moment coefficients in cylinder 3 for radial load at ring 3.

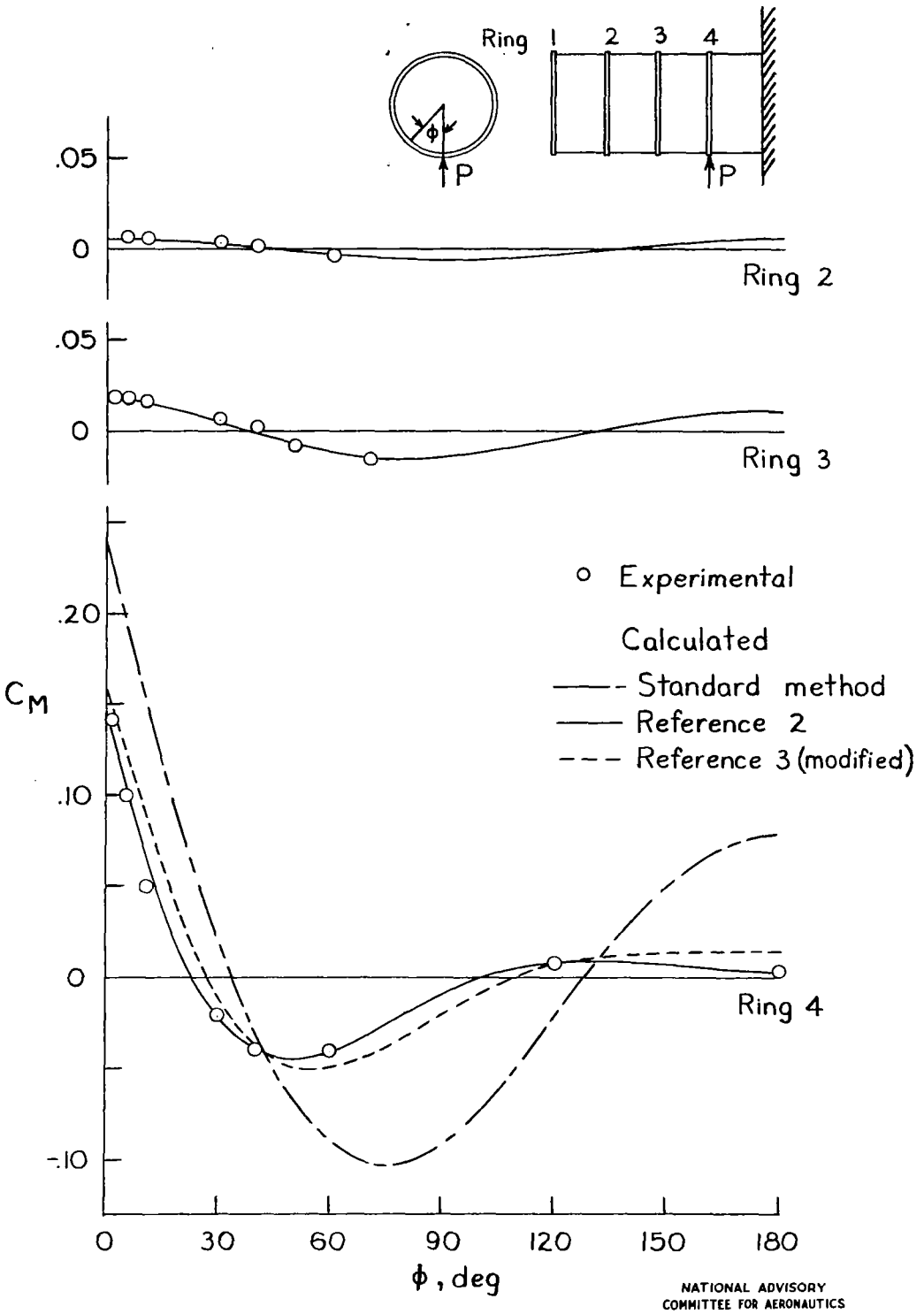

Figure 17. – Ring bending – moment coefficients in cylinder 3 for radial load at ring 4.

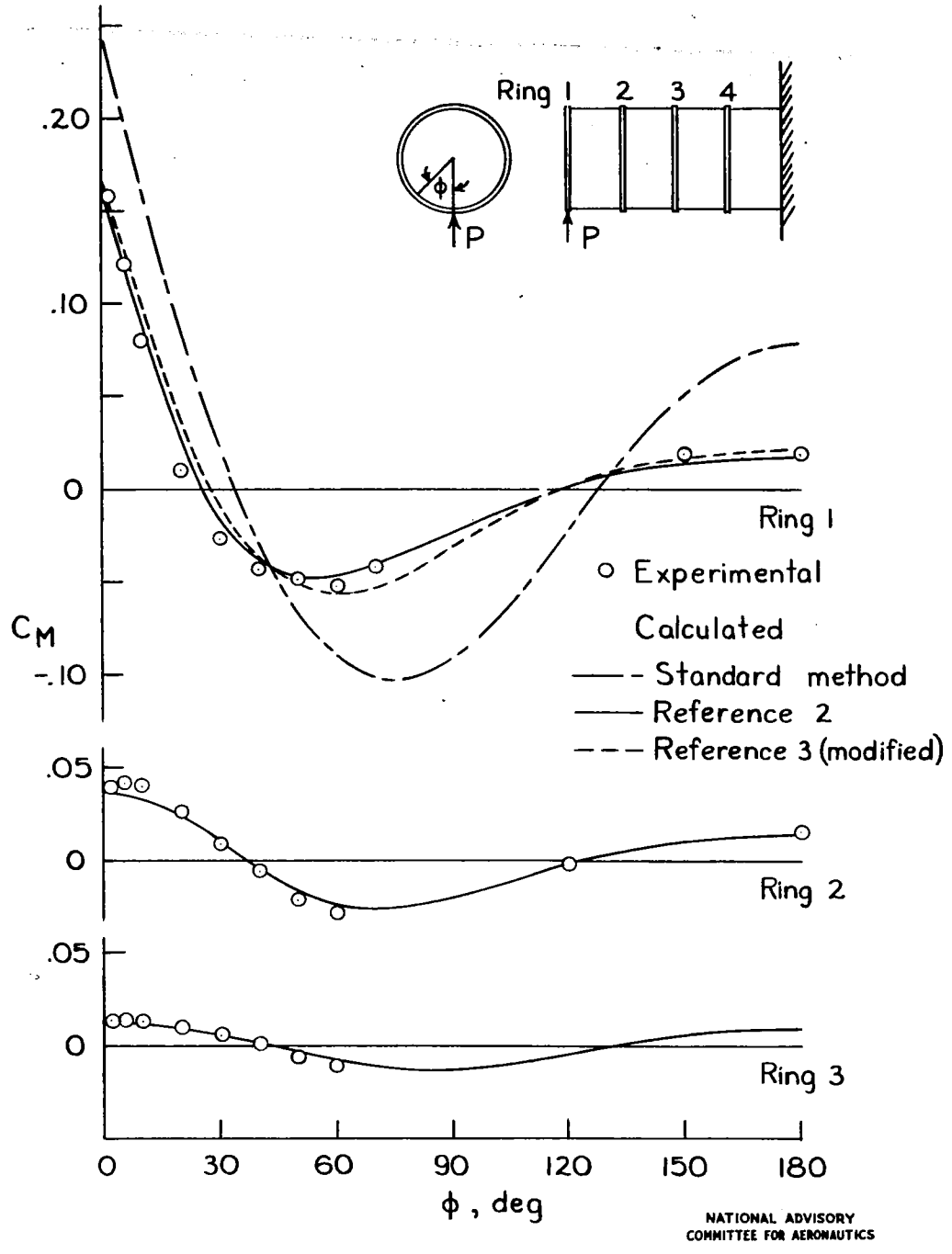

Figure 18.- Ring bending-moment coefficients in cylinder 4 for radial load at ring 1.

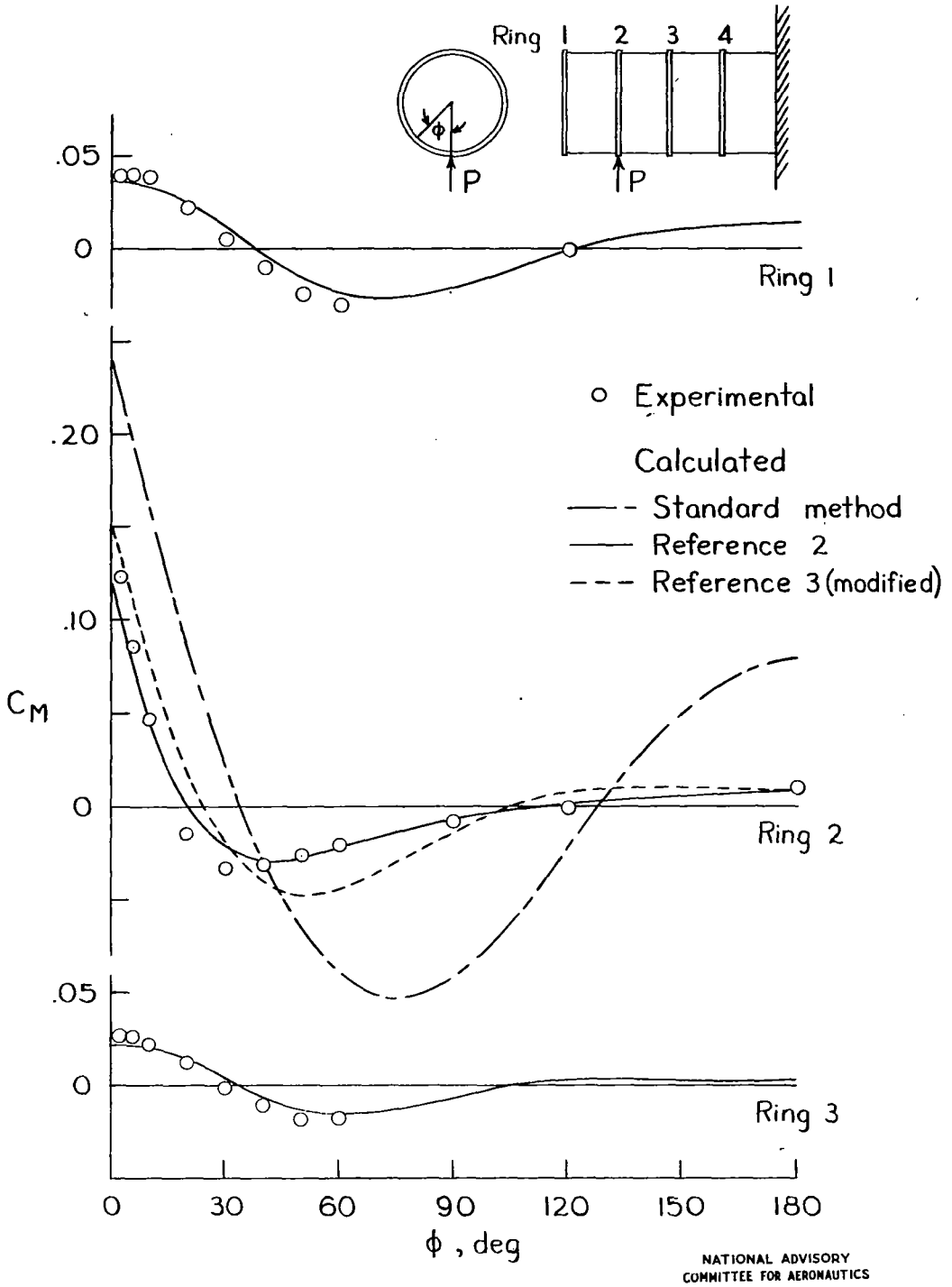

Figure 19.- Ring bending-moment coefficients in cylinder 4 for radial load at ring 2.

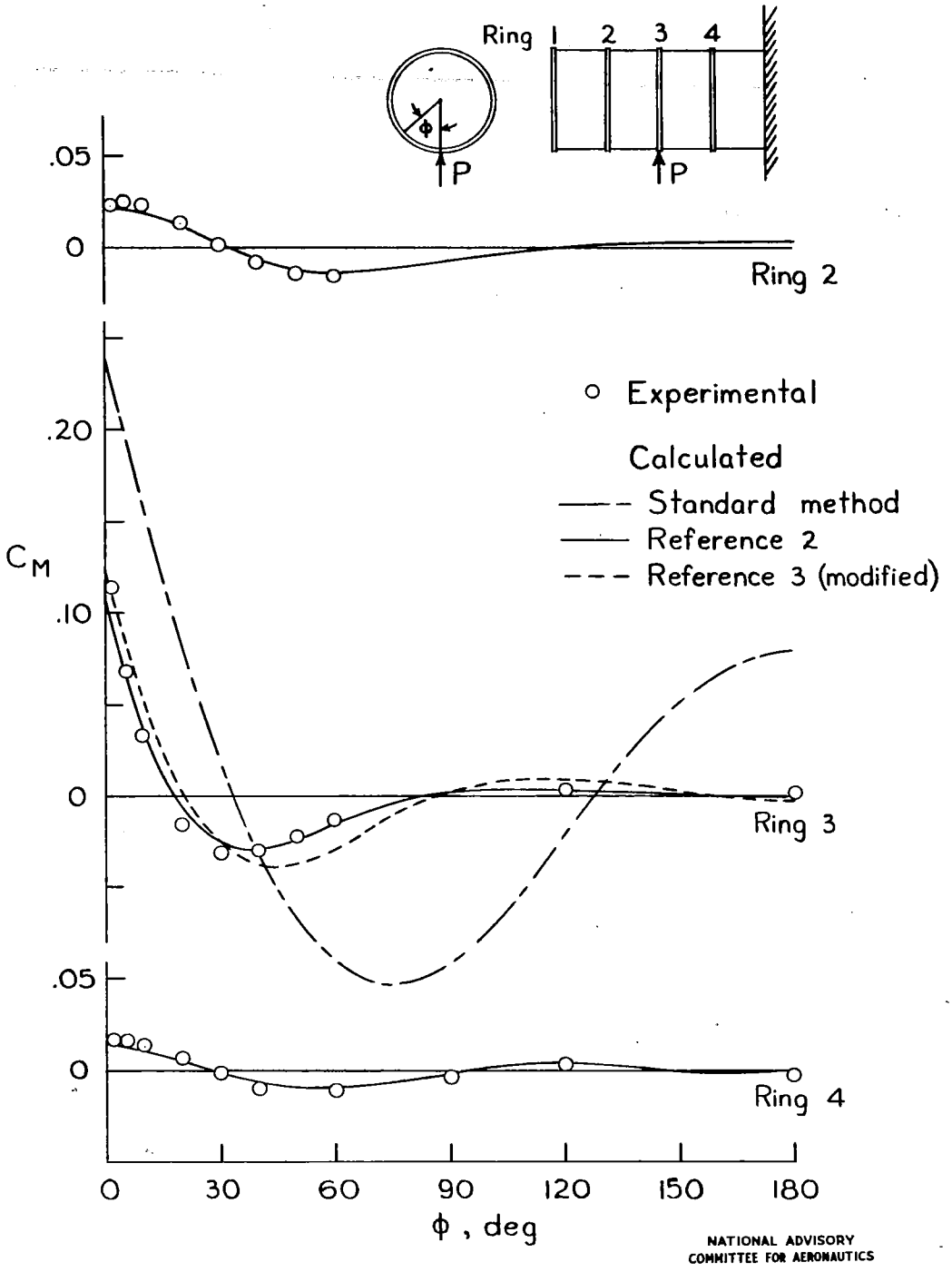

Figure 20.- Ring bending-moment coefficients in cylinder 4 for radial load at ring 3.

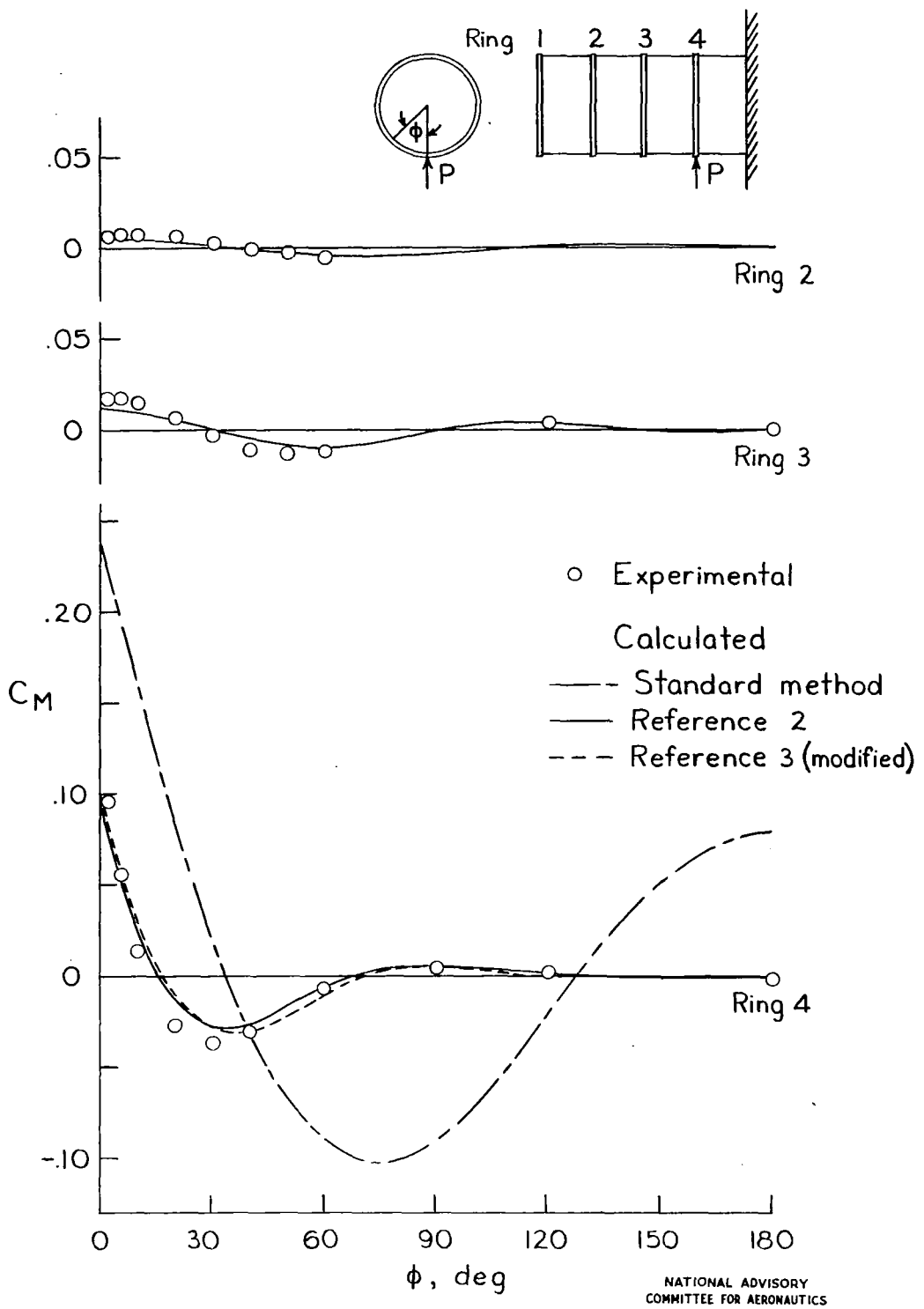

Figure 21.- Ring bending-moment coefficients in cylinder 4 for radial load at ring 4.

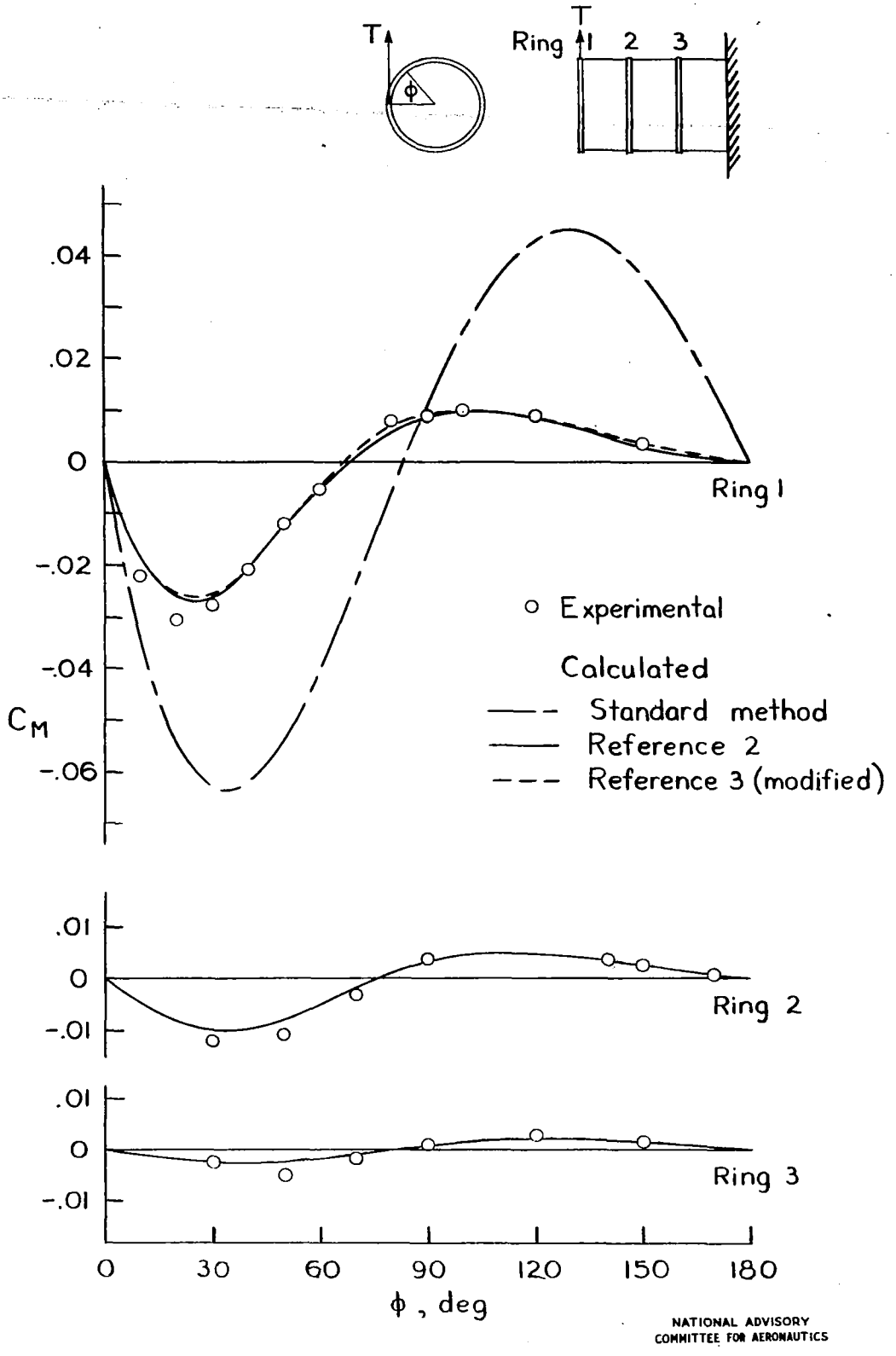

Figure 22.- Ring bending-moment coefficients in cylinder 4a for tangential load at ring 1.

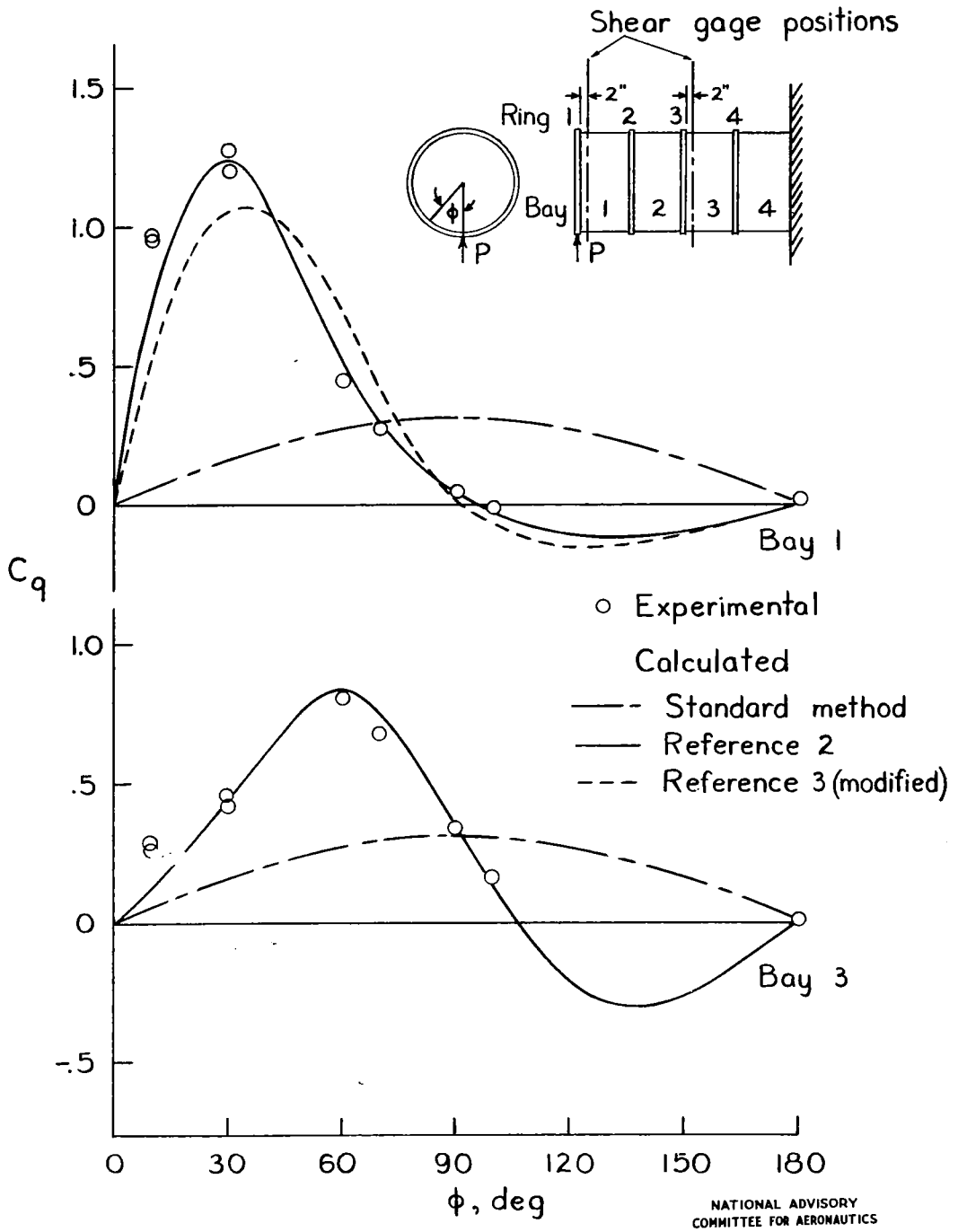

Figure 23. - Shear-flow coefficients in cylinder I for radial load at ring 1.

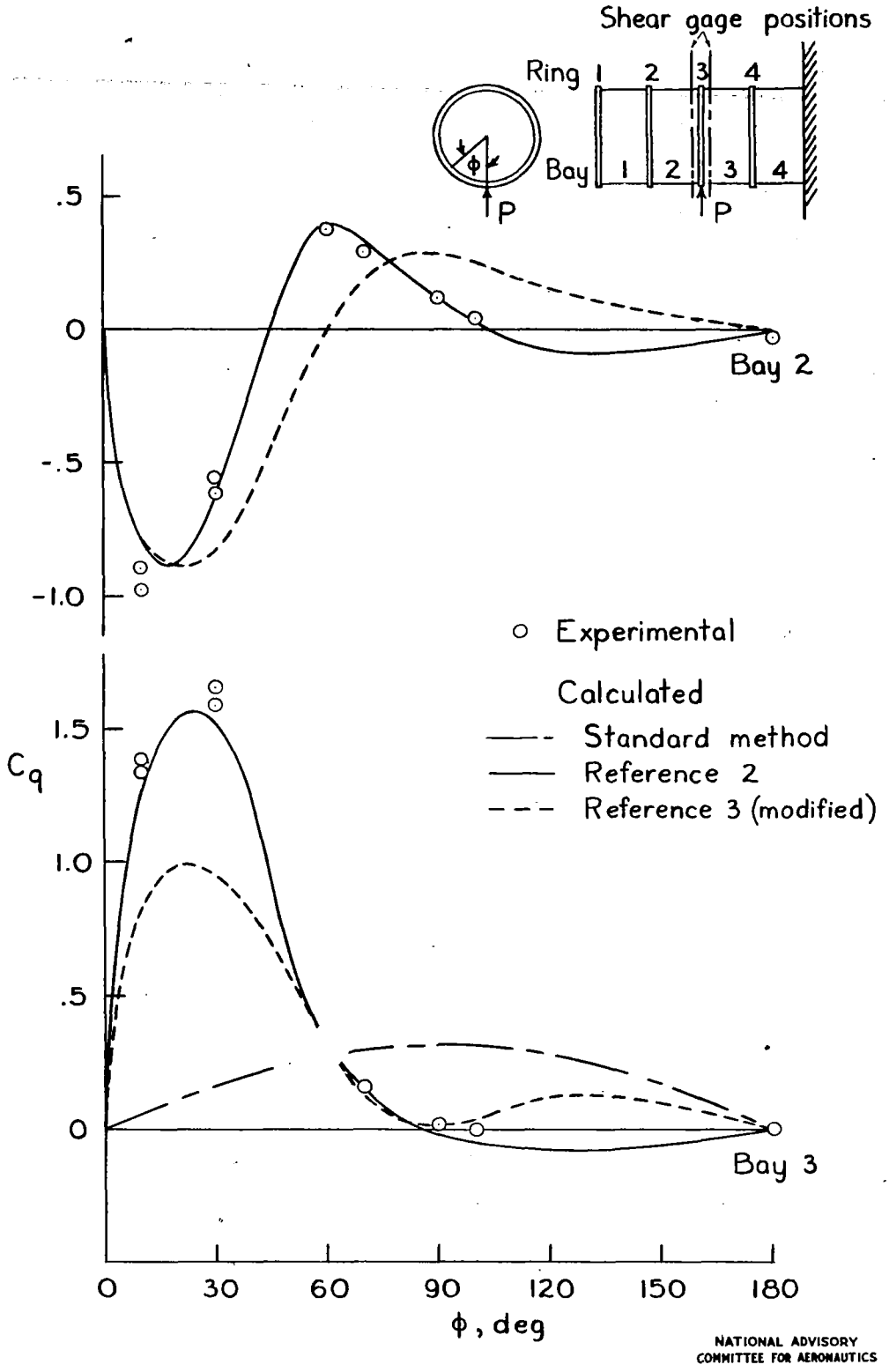

Figure 24.– Shear-flow coefficients in cylinder 1 for radial load at ring 3.

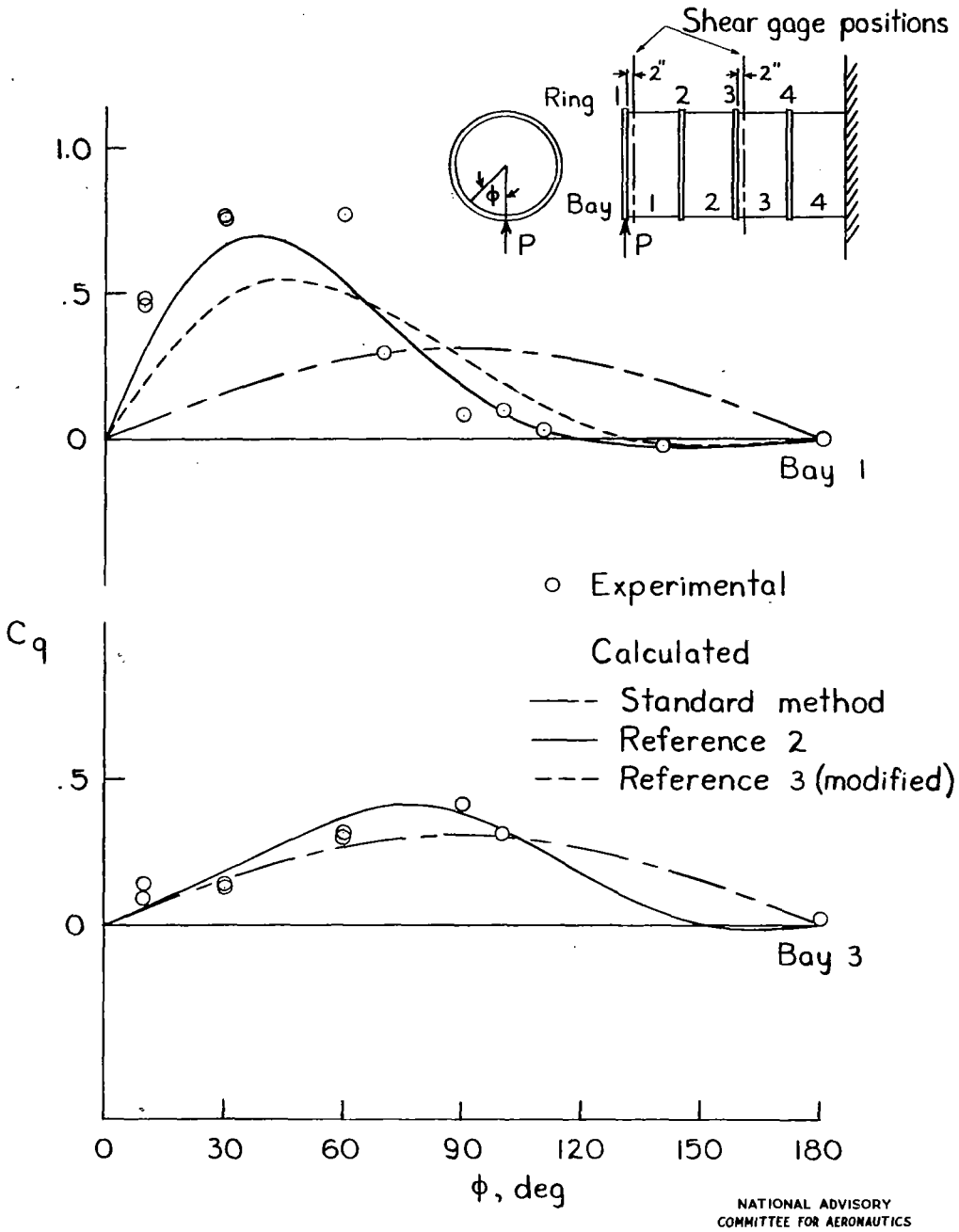

Figure 25.- Shear-flow coefficients in cylinder 2 for radial load at ring 1.

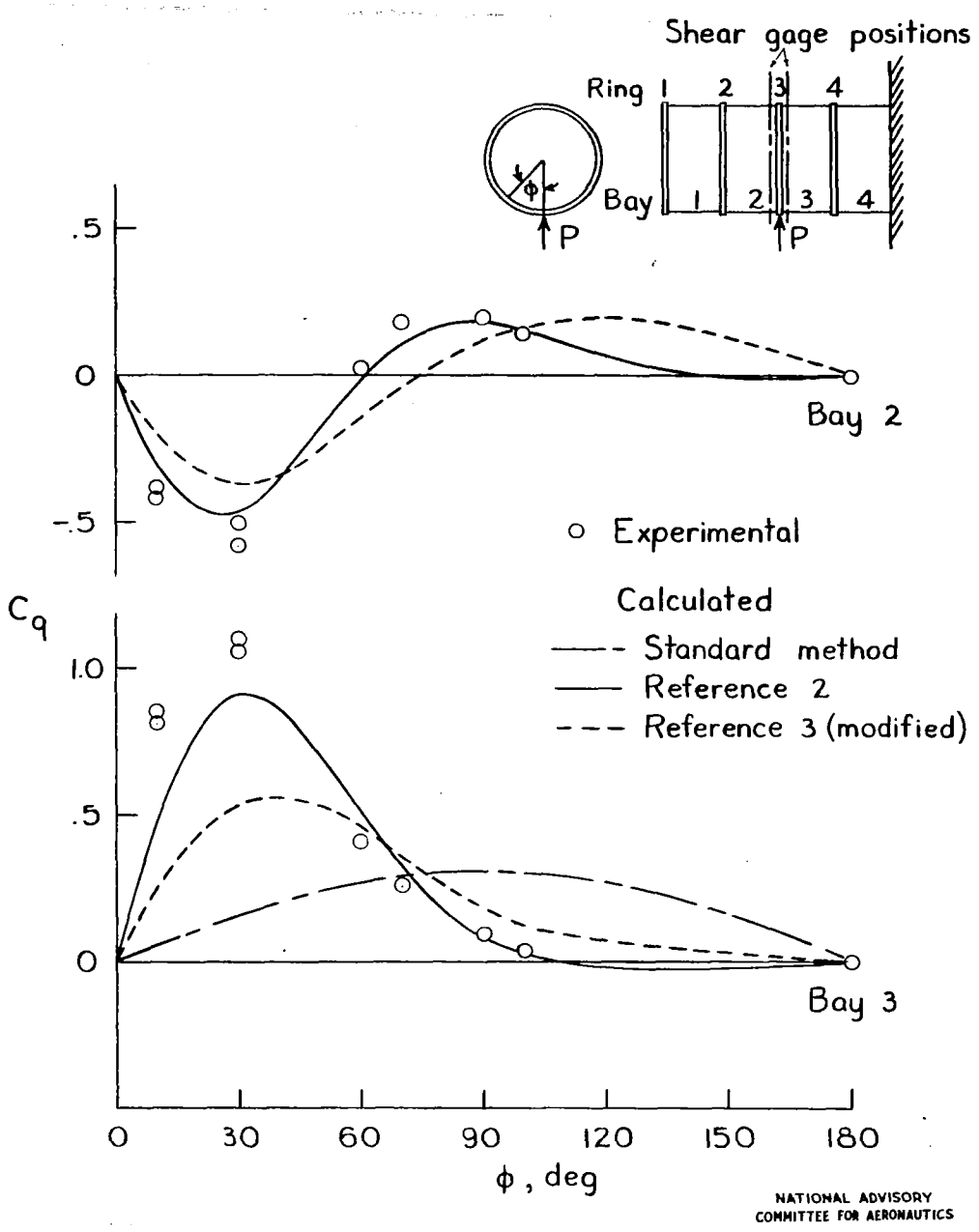

Figure 26.- Shear-flow coefficients in cylinder 2 for radial load at ring 3.

TABLE 1.- DIMENSIONS OF TEST CYLINDERS

Cylinder	Radius of cylinder R (in.)	Length of cylinder (in.)	Spacing of rings L (in.)	Thickness of skin t (in.)	Moment of inertia of ring, I ($in.^4$)
1	15	60	15	0.0322	0.00421
1a	15	60	30	.0322	.00421
1b	15	30	30	.0322	.00421
1c	15	15	15	.0322	.00424
2	15	60	15	.0320	.04001
3	15	60	15	.0320	.35695
4	15	60	15	.0648	.04526
4a	15	45	15	.0648	.04526

NATIONAL ADVISORY
COMMITTEE FOR AERONAUTICS

TABLE 2.- COMPARISONS OF THEORETICAL AND EXPERIMENTAL MAXIMUM BENDING MOMENT COEFFICIENTS

		(1)	(2)		(3)		(4)	(5)				
Cylinder	Loaded ring	C_M Experimental	C_M Computed according to reference 2	d Computed according to reference 3	C_M Computed according to reference 3	d Computed according to reference 3 (modified)	C_M Computed according to reference 3 (modified)	C_M Computed according to standard method	(2)/(1)	(3)/(1)	(4)/(1)	(5)/(1)
Radial load												
1	1	0.123	0.124	10,820	0.071	384.4	0.124	0.239	1.01	0.58	1.01	1.94
	2	.092	.095	10,820	.071	820.8	.109		1.03	.77	1.18	2.60
	3	.083	.086	10,820	.071	2156	.092		1.04	.86	1.11	2.88
	4	.074	.076	10,820	.071	7858	.075		1.03	.96	1.01	3.23
1a	1	.128	.137	10,820	.071	384.4	.124		1.07	.55	.97	1.87
1b	1	.106	.108	10,820	.071	2156	.092		1.02	.67	.87	2.25
1c	1	.082	.086	10,820	.071	7858	.075		1.05	.87	.91	2.91
2	1	.203	.172	1,132	.103	40.2	.181		.85	.51	.89	1.18
	2	.166	.133	1,132	.103	85.8	.157		.80	.62	.95	1.44
	3	.139	.118	1,132	.103	225.5	.135		.85	.74	.97	1.72
	4	.129	.104	1,132	.103	821.9	.109		.81	.80	.84	1.85
3	1	.253	.207	126.9	.147	4.51	.226		.89	.63	.97	1.03
	2	.198	.167	126.9	.147	9.62	.216		.84	.74	1.09	1.21
	3	.183	.160	126.9	.147	25.3	.195		.87	.80	1.07	1.31
	4	.170	.147	126.9	.147	92.1	.155		.86	.86	.91	1.41
4	1	.179	.159	2,026	.093	72.0	.163		.89	.52	.91	1.34
	2	.143	.121	2,026	.093	153.6	.143		.85	.65	1.00	1.67
	3	.132	.109	2,026	.093	403.6	.123		.83	.70	.93	1.81
	4	.122	.097	2,026	.093	1471	.098		.80	.76	.80	1.96
Tangential load												
4a	1	0.031	0.027	2,026	0.011	153.6	0.027	0.064	0.87	0.36	0.87	2.06

NATIONAL ADVISORY
COMMITTEE FOR AERONAUTICS

TABLE 3.- COMPARISONS BETWEEN THEORETICAL AND EXPERIMENTAL MAXIMUM SHEAR FLOW COEFFICIENTS FOR RADIAL LOAD

			(1)	(2)	(3)	(4)	(5)				
Cylinder	Loaded ring	Measured bay	C_q Experimental	C_q Computed according to reference 2	C_q Computed according to reference 3	C_q Computed according to reference 3 (modified)	C_q Computed according to standard method	(2)/(1)	(3)/(1)	(4)/(1)	(5)/(1)
1	1	1	1.24	1.23	3.36	1.15	0.31	0.99	2.71	0.93	0.25
	1	3	.81	.83	3.36	1.15		1.02	4.15	1.42	.38
	3	2	.94	.87	1.63	.92		.93	1.73	.98	.33
	3	3	1.65	1.57	1.73	1.05		.95	1.05	.64	.19
2	1	1	.78	.70	1.60	.60		.90	2.05	.77	.40
	1	3	.37	.42	1.60	.60		1.14	4.32	1.62	.84
	3	2	.55	.47	.72	.41		.85	1.31	.75	.56
	3	3	1.07	.92	.88	.59		.86	.82	.55	.29
3	1	1	.48	.43	.85	.36		.90	1.77	.75	.65
	1	3	.32	.34	.85	.36		1.06	2.66	1.12	.97
	3	2	.27	.25	.32	.16		.93	1.19	.59	1.15
	3	3	.51	.53	.52	.37		1.04	1.02	.73	.61
4	1	1	.90	.80	1.95	.70		.89	2.17	.78	.34
	1	3	.48	.50	1.95	.70		1.04	4.06	1.46	.65
	3	2	.69	.55	.91	.49		.80	1.32	.71	.45
	3	3	1.13	1.07	1.04	.62		.95	.92	.55	.27

NATIONAL ADVISORY
COMMITTEE FOR AERONAUTICS

TABLE 4.- SCHEME OF EQUATIONS FOR CYLINDER OF SIX EQUAL BAYS LOADED AT SECOND RING

$$\left[A = \frac{6R^6t'}{IL^3};\ B = \frac{6Et'R^2}{GtL^2};\ \gamma = \frac{1}{n^2(n^2-1)^2}\right]$$

Coefficients (1) / Equation number	Left-hand side						Right-hand side		
	a_{1n}	a_{2n}	a_{3n}	a_{4n}	a_{5n}	a_{6n}	(Load term)		
	b_{1n}	b_{2n}	b_{3n}	b_{4n}	b_{5n}	b_{6n}	Radial	Tangential	Moment
1	$32n^2 + 2A\gamma + B$	$27n^2 - A\gamma$	$21n^2$	$15n^2$	$9n^2$	$3n^2$	$PA\gamma n/\pi R$	$TA\gamma/\pi R$	$-M_oA\gamma(n^2-1)/\pi R^2$
2	$27n^2 - A\gamma$	$26n^2 + 2A\gamma + B$	$21n^2 - A\gamma$	$15n^2$	$9n^2$	$3n^2$	$-PA\gamma n/\pi R$	$-TA\gamma/\pi R$	$M_oA\gamma(n^2-1)/\pi R^2$
3	$21n^2$	$21n^2 - A\gamma$	$20n^2 + 2A\gamma + B$	$15n^2 - A\gamma$	$9n^2$	$3n^2$	0	0	0
4	$15n^2$	$15n^2$	$15n^2 - A\gamma$	$14n^2 + 2A\gamma + B$	$9n^2 - A\gamma$	$3n^2$	0	0	0
5	$9n^2$	$9n^2$	$9n^2$	$9n^2 - A\gamma$	$8n^2 + 2A\gamma + B$	$3n^2 - A\gamma$	0	0	0
6	$3n^2$	$3n^2$	$3n^2$	$3n^2$	$3n^2 - A\gamma$	$2n^2 + A\gamma + B$	0	0	0

[1]Coefficients a apply to radial load; coefficients b to tangential or moment load.

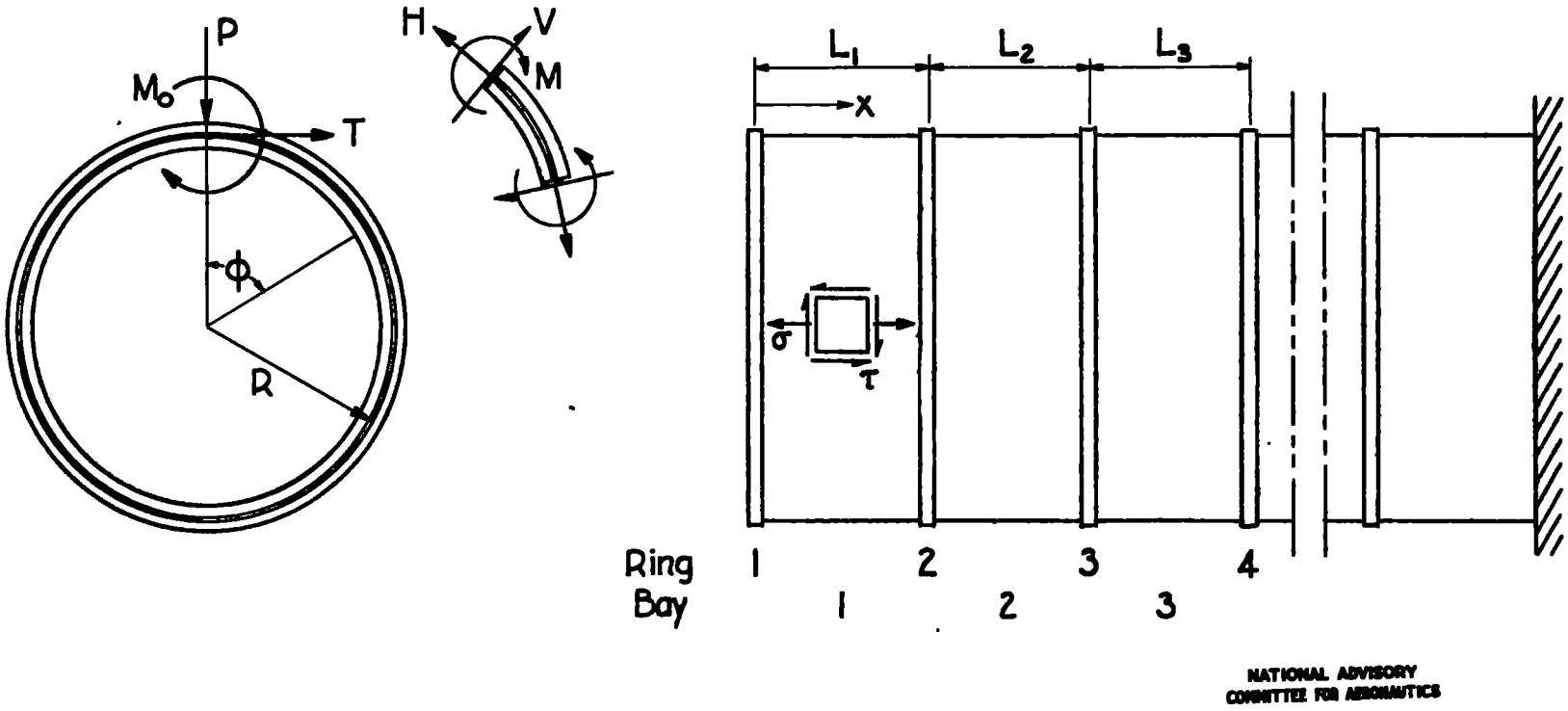

Figure 31.- Symbols and sign convention used in ring analysis.